Astronomy & Astrophysics

Ancient and primordial collisional families as the main sources of X-type asteroids of the inner main belt[*]

Marco Delbo[1], Chrysa Avdellidou[1,2], and Alessandro Morbidelli[1]

[1] Observatoire de la Côte d'Azur, CNRS–Lagrange, Université Côte d'Azur, CS 34229, 06304 Nice Cedex 4, France
e-mail: delbo@oca.eu
[2] Science Support Office, Directorate of Science, European Space Agency, Keplerlaan 1, 2201 AZ Noordwijk ZH,
The Netherlands

ABSTRACT

Aims. The near-Earth asteroid population suggests the existence of an inner main belt source of asteroids that belongs to the spectroscopic X complex and has moderate albedos. The identification of such a source has been lacking so far. We argue that the most probable source is one or more collisional asteroid families that have escaped discovery up to now.
Methods. We apply a novel method to search for asteroid families in the inner main-belt population of asteroids belonging to the X complex with moderate albedo. Instead of searching for asteroid clusters in orbital element space, which could be severely dispersed when older than some billions of years, our method looks for correlations between the orbital semimajor axis and the inverse size of asteroids. This correlation is the signature of members of collisional families that have drifted from a common centre under the effect of the Yarkovsky thermal effect.
Results. We identify two previously unknown families in the inner main belt among the moderate-albedo X-complex asteroids. One of them, whose lowest numbered asteroid is (161) Athor, is ~3 Gyr old, whereas the second one, whose lowest numbered object is (689) Zita, could be as old as the solar system. Members of this latter family have orbital eccentricities and inclinations that spread them over the entire inner main belt, which is an indication that this family could be primordial, that is, it formed before the giant planet orbital instability.
Conclusions. The vast majority of moderate-albedo X-complex asteroids of the inner main belt are genetically related, as they can be included into a few asteroid families. Only nine X-complex asteroids with moderate albedo of the inner main belt cannot be included in asteroid families. We suggest that these bodies formed by direct accretion of the solids in the protoplanetary disc, and are thus surviving planetesimals.

Key words. minor planets, asteroids: general – astronomical databases: miscellaneous

1. Introduction

Collisions in the asteroid main belt are responsible for sculpting the size distribution of these bodies (Bottke et al. 2015a), forming craters on their surfaces, producing fresh regolith (Hörz & Cintala 1997; Basilevsky et al. 2015), ejecting asteroid material into space (Jewitt et al. 2011), and also implanting exogenous materials (McCord et al. 2012; Avdellidou et al. 2018, 2017, 2016; Turrini et al. 2016; Vernazza et al. 2017).

The most energetic impacts can eject asteroid fragments at speeds larger than the gravitational escape velocity of the parent body. This process can form families of daughter asteroids initially placed on orbits that group near that of the parent asteroid (Zappala et al. 1984). Asteroid families can therefore be recognised as clusters of bodies in proper orbital element space – proper semimajor axis, proper eccentricity, and proper inclination (a, e, i) – with significant contrast with respect to the local background (Milani et al. 2014; Nesvorný et al. 2015). The hierarchical clustering method (HCM; Zappalà et al. 1990; Nesvorný et al. 2015, and references therein) is typically used for the identification of these asteroid clusters.

However, family members disperse with time. Dispersion is driven by a change in the a-value ($\mathrm{d}a/\mathrm{d}t \neq 0$) due to the thermal radiation force of the Yarkovsky effect (Vokrouhlický et al. 2006); the eccentricity and inclination are affected by orbital resonances with the planets, the locations of which are crossed by the asteroids as they drift in semimajor axis. This process has fundamental consequences: families older than ~2 Gyr tend to lose number density contrast with respect to the local background population (Parker et al. 2008; Spoto et al. 2015; Carruba et al. 2016). They become more difficult to detect using the HCM compared to younger ones (Walsh et al. 2013; Bolin et al. 2017; Delbo et al. 2017). In addition to the effect of orbital resonances currently present in the main belt, the scattering of fragments of primordial families (Milani et al. 2017, 2014; Delbo et al. 2017) was also affected by major dynamical events such as the giant planet orbital instability, which is shown to have happened at some point in the solar system history (Morbidelli et al. 2015). This latter instability shifted the positions of the resonances and resulted in the incoherent dispersion of e and i of any pre-existing primordial asteroid family in the main belt (Brasil et al. 2016), as is the case for the family of low-albedo asteroids found by Delbo et al. (2017) in the inner main belt (i.e. $2.1 < a < 2.5$ au).

The sign of $\mathrm{d}a/\mathrm{d}t$ depends on the obliquity of the spin vector of the asteroid, with prograde-rotating asteroids drifting with $\mathrm{d}a/\mathrm{d}t > 0$ and retrograde ones with $\mathrm{d}a/\mathrm{d}t < 0$. To first order, the

---

[*] This work is dedicated to the memory of Andrea Milani, who put the foundation and devoted his scientific career on the study of asteroid families.

value of da/dt is inversely proportional to the diameter D of family members, such that at any given epoch, the orbits of smaller asteroids are moved further away from the centre of the family than the bigger ones are. Due to this mechanism, an asteroid family forms a characteristic shape in the space of proper semi-major axis a versus inverse diameter ($a, 1/D$), which is called V-shape as the distribution of asteroids resembles the letter "V" (Milani et al. 2014; Spoto et al. 2015; Bolin et al. 2017). The slopes of the borders of the "V" indicate the age of a family (see e.g. Spoto et al. 2015), with younger ones having steeper and older ones shallower slopes. While orbital resonance crossings produce diffusion of e and i, these have minimal effect on a (Milić Žitnik & Novaković 2016), resulting in the conservation of the V-shape of families for billions of years. The semimajor axis values can only be modified by gravitational scattering due to close encounters with massive asteroids (Carruba et al. 2013; Delisle & Laskar 2012) or in the case that a planet momentarily entered the main belt during the orbital instability phases of the giant planets (Brasil et al. 2016). The former effect has been shown to be negligible for families with ages of approximately 1 Gyr (Delbo et al. 2017). The second case did not happen for the inner main belt; if it had, the V-shape of the primordial family discovered by Delbo et al. (2017) would not be visible.

Another fundamental consequence of the a-mobility due to the Yarkovsky effect is that asteroids can drift into powerful mean motion or secular orbital resonances with the planets, causing these bodies to leave the main belt. These escaping asteroids can reach orbits in the inner solar system, eventually becoming near-Earth asteroids (NEAs; Morbidelli & Vokrouhlický 2003). It would be useful to trace back the orbital evolution of NEAs and find their place of origin in the main belt. Unfortunately, this is not possible in a deterministic way due to the chaotic nature of their orbital evolution. Still, not all the information is lost, and methods have been developed to identify the source region of NEAs in a statistical sense (Bottke et al. 2002; Granvik et al. 2017, 2016; Greenstreet et al. 2012). For each NEA, the probability of originating from different source regions, which include the main belt, the Jupiter family comets (JFC), the Hungaria (HU) and the Phocaea (PHO) populations, is calculated. It is found that the most efficient route from the main belt to near-Earth space is offered by the family formation in the inner main belt and delivery through the ν_6 resonance complex (Granvik et al. 2016) or – to a lesser extent – the J3:1 mean motion resonance (MMR) with Jupiter.

On the basis of the source-region probabilities, osculating orbital elements, spectral classes, and albedos, different studies have attempted to match properties of notable NEAs with their main-belt family counterparts. For instance, the NEA (3200) Phaethon, which is associated with the Geminids meteor stream (Fox et al. 1984; Gustafson 1989; Williams & Wu 1993), has been linked to the Pallas family (de León et al. 2010; Todorović 2018); (101955) Bennu, the target of NASA's OSIRIS-REx sample return mission (Lauretta et al. 2012), is likely coming from one of the low-albedo, low-orbital-inclination families of the inner main belt, such as Eulalia or Polana (Bottke et al. 2015b; Campins et al. 2010). The target of JAXA's Hayabusa2 sample return mission (162173) Ryugu, also identified as 1999 JU$_3$, was linked to the Polana family (Campins et al. 2013) or the low-albedo asteroid background of the inner main belt. The latter was later suggested to form a family by itself that could be as old as the solar system (Delbo et al. 2017). The discovery of the aforementioned primordial family implies that the background of low-albedo unaffiliated asteroids in the inner main belt is represented by only a few asteroids, all larger than ∼50 km in diameter. This means that the smaller low-albedo asteroids of the inner main belt could be genetically linked to a few distinct asteroid parents (Delbo et al. 2017) and that the low-albedo NEAs with a high probability of coming from the inner main belt are also linked to these few distinct asteroid parents. These later findings are also independently confirmed by the work of Dermott et al. (2018).

On the other hand, concerning the NEAs with high albedo ($p_V > 0.12$) and not those belonging to the spectroscopic C-complex, the situation is less clear. Nonetheless, several important S-complex families in the inner main belt are known that could be the source of NEAs belonging to the same spectroscopic complex. For instance, the Flora family (Vernazza et al. 2008) is capable of delivering NEAs belonging to the S complex and with composition similar to the LL ordinary chondrite meteorites (Vokrouhlický et al. 2017). Moreover, Reddy et al. (2014) propose that the Baptistina asteroid family is the source of LL chondrites that show shock-blackened impact melt material.

The NEA population also contains a significant number of X-complex asteroids (Binzel et al. 2015), whose origin remains unclear despite their link with meteorites and asteroids being visited by space missions (see Sect. 2).

This work focuses on the search for X-type families in the inner main belt, which could represent sources of X-type NEAs, in particular those with intermediate albedo. Dykhuis & Greenberg (2015) have already noted the presence of a small X-type family that they call Hertha-2, that could produce some NEAs. However, this latter family is arguably too small to account for the flux of the observed X-type NEAs. In Sect. 2 we describe the main physical properties of X-complex asteroids. In Sect. 3 we analyse the source regions of X-type NEAs and show that the inner main belt has a significantly higher probability of delivering X-type asteroids to the near-Earth space compared to other areas of the solar system. In Sects. 4 and 5 we describe our search for and identification of families amongst X-type asteroids of the inner main belt, and in Sect. 6 we present the implications of our findings.

2. Characteristics of the spectroscopic X complex

The spectroscopic X complex is characterised by moderately sloped spectra with no or weak features and is compositionally degenerate, as it contains objects with high, medium, and low albedos (Fornasier et al. 2011; DeMeo et al. 2015). For instance, the X complex in the Tholen taxonomy (Tholen & Barucci 1989) is primarily separated into the E-, M-, and P-types which have different albedo ranges (see Fig. 1). According to the more recent Bus-DeMeo taxonomy (DeMeo et al. 2009), the X complex contains the Xe, Xc, and Xk classes with very different inferred mineralogies. Spectroscopically, these classes are very close to some C-complex classes, such as the Cg, Ch, and Cgh, and therefore a more detailed analysis of their specific features is needed (DeMeo et al. 2009). The low-albedo X-complex asteroids could be compositionally similar to those of the C complex (DeMeo et al. 2009, 2015). An indication of the composition similarities and origin between the low-albedo asteroids belonging to the X and C complexes also comes from the fact that X- and C-complex asteroids have been found within the same families (Morate et al. 2016; Fornasier et al. 2016). In the near-infrared survey of Popescu et al. (2018), asteroids belonging to the X complex are denoted by the class Xt.

The high albedo E-types ($p_V > 0.3$) are represented by the Xe-type asteroids and have a flat spectrum with a weak absorption band at 0.9 μm and a deeper one at 0.5 μm
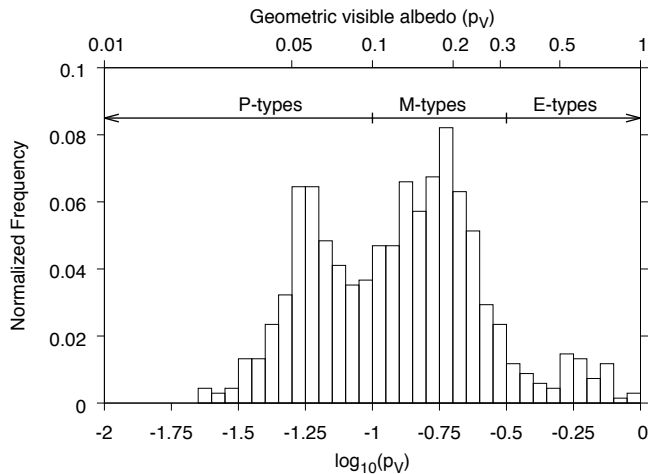
Fig. 1. Multimodal distribution of the geometric visible albedo of all asteroids belonging to the X complex (i.e. with spectral types found in literature being X, Xc, Xe, Xk, M, E, and P). The three peaks of the distribution correspond to the P-, M-, E-types of the Tholen & Barucci (1989) taxonomy, and their boundaries are defined $p_V \leq 0.1$, $0.1 \leq p_V \leq 0.3$, and $p_V > 0.3$, respectively, and are marked by the arrows at the top of the figure. As one can see these albedo boundaries provide reasonable separation between the classes. In this work we focus on X-complex asteroids with $0.1 \leq p_V \leq 0.3$, that is, the M-types of Tholen & Barucci (1989), which in Bus-DeMeo mostly corresponds to the Xc-types.

(DeMeo et al. 2009). They have been compositionally linked to the enstatite achondrite (aubrites) meteorites (Gaffey et al. 1992; Fornasier et al. 2008) and their main reservoir at small heliocentric distances is found in the Hungaria region at high inclination (Gaffey et al. 1992; Ćuk et al. 2014); in particular they are members of the Hungaria family, which is superimposed on an S-complex dominated background (Lucas et al. 2017).

The traditional Tholen & Barucci (1989) M-type group, with moderate albedo range ($0.1 < p_V < 0.3$), has been shown to contain objects with several compositions, including metallic objects of iron/nickel composition, thought to be the parent bodies of the iron meteorites and supposed to represent the cores of differentiated objects. In the Bus-DeMeo taxonomy moderate albedo asteroids belong to the Xk and Xc classes. In particular, it has been shown that asteroids classified as Xk are compositionally linked to the mesosiderite meteorites; in particular with asteroids (201) Penelope, (250) Bettina, and (337) Devosa (Vernazza et al. 2009). Xc-type asteroids, having a reflectance spectrum with the shallowest slope compared to the rest X-complex asteroids in the range 0.8–2.5 μm, constitute the only asteroid class of the X complex that is characterised by the absence of the 0.9 μm feature, the latter being linked to the presence of orthopyroxene (Hardersen et al. 2005). Asteroids of the Xc class have been linked to the enstatite chondrite (EC) meteorites. Two characteristic Xc-types are (21) Lutetia and (97) Klotho (Vernazza et al. 2009).

On the other hand, P-types, the dark asteroids of the X-types, are not well represented in the newer taxonomy. They are located mainly in the outer belt and are similar to C-complex asteroids, being also linked with CM meteorites (Fornasier et al. 2011).

From the currently available data there are two Xk asteroids, (56) Melete and (160) Una, and one Xc asteroid, (739) Mandeville, which all have very low albedo values showing that there is no strict matching between the medium albedo M-types and the Xc/Xk-types.

3. Source regions of X-type NEAs

For our study we extract asteroid information from the Minor Planet Physical Properties mp3 Catalogue[1], developed and hosted at Observatoire de la Côte d'Azur. This database contains orbits and physical properties of both MBAs and NEAs. Specifically, for NEAs it also includes albedo and spectral classes obtained from the Data Base of Physical and Dynamical Properties of Near Earth Asteroids of the E.A.R.N. (European Asteroid Research Node) hosted by the DLR Berlin.

We select NEAs of the X-, Xk-, Xc-, Xe-, E-, M-, and P-types according to Tholen (Tholen & Barucci 1989), Bus (Bus & Binzel 2002), and Bus-DeMeo (DeMeo et al. 2009) taxonomies. As a second filter we require their geometric visible albedo (p_V) to be in the range $0.1 < p_V < 0.3$. This albedo cut excludes the bright Xe-types, mostly linked to the Hungaria region, and the dark X-type population probably linked to carbonaceous asteroids. We note that P-types had, by definition, $p_V < 0.1$ in the taxonomy of Tholen & Barucci (1989). However, some of the p_V values have been revised since the original work of Tholen & Barucci (1989), making it possible that some P-types could have revised $p_V > 0.1$; we find no such cases however.

For each NEA that passes our selection criteria – 15 asteroids in total – we extract its source region probabilities, which we take from the work of Granvik et al. (2016, 2017). In this model there are seven source regions for the NEAs; the Hungaria (HU) and Phocaea (PHO), the J3:1, J5:2 and J2:1 MMR, the Jupiter-family comets (JFC) and the ν_6 complex, the latter including the ν_6 secular resonance, and the J4:1 and J7:2 MMR. We take the mean of the source probabilities for the considered NEAs and display the results in Fig. 2, which shows that the ν_6 source dominates, with the second most effective source region being the J3:1. The latter could also contribute with asteroids drifting inward from the central main belt ($2.5 < a < 2.82$ au). The J4:1 MMR and the ν_6 secular resonance determine the inner border of the main belt, while the J7:2 that overlaps with the M5:9 MMR at a heliocentric distance of 2.256 au also delivers to near-Earth space asteroids from the inner portion of the main belt (see also Bottke et al. 2007).

The average size (diameter) of the selected NEAs, calculated to approximately 1.5 km, implies that these bodies are very unlikely to be planetesimals that formed 4.567 Gyr ago. This is because their size-dependent collisional lifetime is <1 Gyr (Bottke et al. 2005). In addition, there is evidence that the planetesimals, that is, the original asteroids, were much bigger, possibly with sizes around 100 km (Morbidelli et al. 2009) and a shallow size distribution (Tsirvoulis et al. 2018); they were certainly bigger than a few tens of kilometres in diameter (35 km, see Delbo et al. 2017). The aforementioned argument implies that these NEAs originate from a more recent fragmentation of a larger parent that formed a family. Slowly the family members drifted by the Yarkovsky effect into one of the source regions, which removed them from the main belt and delivered them to the near-Earth space.

The question that arises pertains to the identity of the potential families that feed the NEA population with X complex objects with moderate albedo. The most well-known X-complex family is Hungaria in the Hungaria region. However, as described earlier, this has several Xe-type asteroids with high albedo values of $p_V > 0.3$ that have been discarded by our filtering criterion. In the inner main belt there are five families

---

[1] mp3c.oca.eu
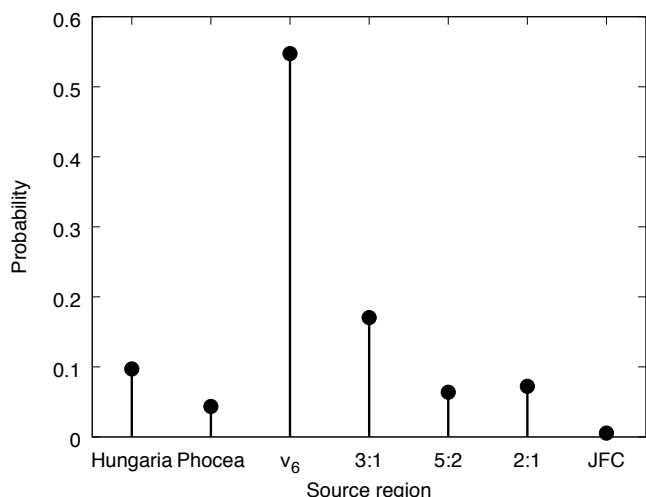
Fig. 2. Source regions of the 15 selected NEA that fulfil the criteria in spectral class and albedo range. The region with the highest probability on average is the ν_6, indicating that the source should be the inner main belt.

that are characterised in the literature as X or CX-type: Clarissa, Baptistina, Erigone, Chimaera and Svea (Nesvorný et al. 2015). Closer inspection of the family members of Clarissa (introduced as an X-type) shows that they have very low albedos (average family albedo is $p_V = 0.05$) consistent with a P-type classification in the Tholen & Barucci (1989) taxonomy. The asteroid (302) Clarissa itself is classified as an F-type, and in visible wavelengths is spectroscopically similar to (142) Polana (another F-type), the potential parent body of the Polana family (Walsh et al. 2013). Therefore, it is more appropriate to consider Clarissa as a family with a carbonaceous composition. The Erigone family has an average albedo of $p_V = 0.06$, while the few objects that have been classified as X or CX-type have very low albedos ($p_V < 0.08$), indicating that this family also has very likely a carbonaceous composition. Likewise, Svea also has a carbonaceous composition, because the average and standard deviation of the albedo distribution of its members are $p_V = 0.06$ and 0.02, respectively. The only member of the Svea family classified as an X-type is (13977) Frisch that has $p_V = 0.16 \pm 0.02$, which is 5σ from the mean. This could be an indication that this asteroid is an interloper and in reality does not belong to the Svea family. Chimaera, with an average of $p_V = 0.07$ and a standard deviation of 0.05, has 108 asteroid members of which eight have been indicated either as CX or as C and X (in different taxonomies). This indicates that this family also cannot produce moderate albedo X-type NEAs.

The Baptistina asteroid family is young ($t < 300$ Myr, Brož et al. 2013), contains almost 2500 members (Nesvorný et al. 2015) of moderate albedos (mean $p_V = 0.16$), and is capable of delivering objects in the near-Earth space (Bottke et al. 2007). According to spectroscopic and spectrophotometric observations, 417 family members have been classified, of which 154 as S-types, 172 as C or CX-types (or simultaneously C and X), while only 18 X-types. The asteroid (298) Baptistina itself is spectroscopically classified as an Xc-type object. A recent study has classified (298) Baptistina as S-type and suggests that it is the parent body of the Chelyabinsk bolide (Reddy et al. 2014), which hit Earth's atmosphere on February 13, 2013. Chelyabinsk meteorites, which resulted from the bolide, match the composition of the LL ordinary chondrite meteorites. In general, LL chondrites are linked to S-type asteroids, and the most prominent family

spectroscopically similar to LL chondrites is Flora. However, analysis of 11 members of the Baptistina family show spectra akin to those of LL5 chondrites, but with lower albedos compared to typical S-types. This lower albedo can be explained by the presence of blackening impact melts (Reddy et al. 2014). Baptistina and Flora families overlap in the orbital element space and whether or not the Baptistina family was formed by the breakup of a once-upon-a-time Flora member remains an open question (Nesvorný et al. 2015).

From the above considerations, there is no solid evidence for the presence of an inner main-belt X-type family with moderate albedos that is also the source of Xc/Xk NEAs. Since moderate-albedo X-complex asteroids have been observed in near-Earth space and originate from the inner main belt it is possible that one or more diffused families of X-types with moderate albedos have so far escaped identification by classical family-searching methods such as the HCM. In the following, we use a new method (Bolin et al. 2017), already successfully tested (Delbo et al. 2017), to search for the missing X-type families in the inner main belt.

4. Materials and methods

4.1. Selection of asteroids

We restricted our search for the intermediate albedo component of the X complex (see Fig. 1) and thus we select all asteroids of the inner main belt (with $2.1 < a < 2.5$ au) with $0.1 \leq p_V \leq 0.3$ belonging to the X complex and with spectral taxonomic classes of X, Xc, Xe, Xk, Xt, M, E, as described in Sect. 2. We also checked for Tholen & Barucci (1989) P-types in the IMB, which could have a revised $p_V > 0.1$, finding no such cases. This selection resulted in a pool of 386 asteroids.

We used the database of Delbo et al. (2017), which can now be accessed from the mp3 Catalogue[1] (see Sect. 3), to perform these extractions. The database was used to extract proper orbital elements and diameter values for the selected asteroids on which we apply the family searching technique. In this database, all known asteroids as of 2016 November 4 from the Minor Planet Center[2], are crossmatched with (i) the synthetic and analytic (for those asteroids without synthetic) proper elements Milani et al. (2014) of the AstDys-2 database[3]; (ii) radiometric diameters and albedos taken from Nugent et al. (2016, 2015), Masiero et al. (2012a, 2011, 2014), Tedesco et al. (2002), Ryan & Woodward (2010), and Usui et al. (2011) combined in reverse order of preference (i.e. results from a latter reference in the order presented here overwrite those of a preceding one, in order to have a unique diameter and albedo value for each asteroid); (iii) spectral classification from several sources (Neese 2010; Carvano et al. 2010; DeMeo & Carry 2013; de León et al. 2016); and (iv) rotational periods from the Asteroid Lightcurve database (Warner et al. 2009).

4.2. Family search method

Since our working hypothesis is that a putative missing X-complex family is dispersed and therefore very likely old, we use the method of Bolin et al. (2017) to search for Yarkovsky V shapes of families in the inner main belt. This technique searches for V shapes of unknown age and vertex in an asteroid population, in the 2D space of parameters representing the centre of the family, a_c, and the slope, K, of the sides of the V shape.

[2] https://www.minorplanetcenter.net, downloaded Nov 2016.
[3] http://hamilton.dm.unipi.it/astdys/

To do so, the method draws in the $(a, 1/D)$ space a nominal-V described by the equation $1/D = K|a - a_c|$, an inner V with equation $1/D = (K - \Delta K)|a - a_c|$, and an outer V with equation $1/D = (K + \Delta K)|a - a_c|$. Subsequently, we count how many asteroids fall in between the borders of the inner- and the nominal V and between the borders of the nominal- and the outer V, noted N_{in} and N_{out}, respectively. The value of N_{in}^2/N_{out} is then plotted as a function of a_c and K. Local maxima of N_{in}^2/N_{out} indicate V-shaped over-densities of asteroids which may be associated to a Yarkovsky-evolved asteroid family.

In order to determine the uncertainties on the values of K and a_c, we improve the technique used by Delbo et al. (2017), who adopted the method of Spoto et al. (2015), by using here a more rigorous approach. First of all, since our selection of asteroids depends on the values of their geometric visible albedos being within the aforementioned limits ($0.1 \leq p_V \leq 0.3$), we perform 10^4 Monte Carlo simulations where the nominal values of the albedos and diameters of asteroids are varied within their uncertainties, which are assumed to be 1σ values drawn from Gaussian distributions. At each iteration, a new selection is performed based on the albedo range and a new V-shape search is performed around the nominal centre and slope of the V shape and the values of a_c and K of each iteration that maximise N_{in}^2/N_{out} are recorded. The RMS of the distributions of the recorded a_c and K are taken as the uncertainties on those parameters.

4.3. Statistical tests

Following the method of Delbo et al. (2017) we assess whether a V-shape distribution of asteroids could be due to statistical sampling instead of indicating the existence of a real V-shaped over-density, characteristic of an asteroid family. To do so, we perform a statistical test where we assume the null hypothesis that the distribution of the values of the proper semimajor axis is size independent. This null hypothesis would mean that the asteroids are neither genetically related nor dispersed by the Yarkovsky effect from a common centre. Subsequently, for each asteroid we preserve its diameter value and assign a new proper semimajor axis. This value of a is randomly extracted each time from the proper semimajor axis distribution of all X-complex asteroids of the inner main belt with $0.1 < p_V < 0.3$ regardless of their size. We typically perform 10^6 iterations and we measure in which fraction of the trials we generate a V shape as the one observed, that is, the fraction of the simulations with a number of asteroids falling outsize our nominal V-shape borders that is smaller or equal to the observed one. If we find, for instance, that in 68.27 or 99.73% of the simulations the number of asteroids outsize the V-shape borders is smaller or equal to the observed one, respectively, which implies that the existence of the family is robust at 1 and 3σ, respectively.

4.4. Identification of a family core

Once a V shape is located (as e.g. in Fig. 3), we also attempt to determine whether the distributions of the orbital eccentricity and inclination of the asteroid population near and inside the borders of the V shape have peaks, possibly indicating orbital clustering of the family members. To do so, we plot the distribution of the number of asteroids in bins of eccentricity and inclination normalised by the amount of orbital phase space available in each bin. For the case of the eccentricity, the available a-space between the Mars-crossing boundary and the J3:1 MMR decreases with increasing $e > 0.2$. This is because
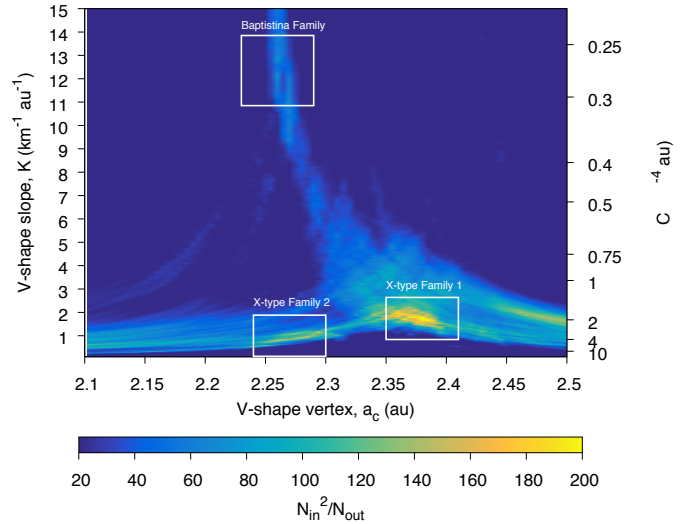
Fig. 3. Output of the V-shape-searching method. The value of N_{in}^2/N_{out} is plotted as a function of the slope (K) and semimajor axis of the vertex of a V shape (a_c). The value of the parameter C, which measures the width of a V shape in the (a, H) space, where H is the absolute magnitude (Vokrouhlický et al. 2006) and is calculated from $C = 1/K \sqrt{p_V}/1329$ using a geometrical visible albedo $p_V = 0.2$.

asteroids with $e > 0.2$ and $2.1 < a < 2.5$ au can have perihelion distances, $q = a(1 - e)$, below the aphelion distances of Mars ($Q_{Mars} = 1.666$ au). For the lower ($e_{l,j}$) and upper limit ($e_{h,j}$) of each jth-bin of e, we compute their corresponding a-values ($a'_{l,j}$ and $a'_{h,j}$) using Eq. (1) that represent the Mars-crossing curve:

$$a' = 2.1 \qquad \text{for } e \leq 1 - Q_{Mars}/2.1,$$
$$a' = 1 - Q_{Mars}/(1 - e) \quad \text{for } e > 1 - Q_{Mars}/2.1. \tag{1}$$

We then compute the area of the trapezium-shaped a space between the Mars-crossing curve and the J3:1 MMR of the inclination bin:

$$\text{area}'_j = (a'_{l,j} - 2.5 + a'_{h,j} - 2.5) \times (e_{h,j} - e_{l,j})/2. \tag{2}$$

Figure 4 shows that the distribution of X-type asteroids with $0.1 \leq p_V \leq 0.3$ of the IMB is probably unaffected by the Mars-crosser border, but we prefer to include it for the sake of generality of the method. For the case of the inclination, the available a-space between the ν_6 and the J3:1 MMR decreases with increasing inclination, as the a-value of centre of the ν_6 varies from ~ 2.1 au at $\sin i = 0$–2.5 au for $\sin i = 0.31$. We approximate the shape of the ν_6 with a second-order polynomial of the form:

$$a = A \sin^2 i + B \sin i + C, \tag{3}$$

where $A, B,$ and C have the values 4.99332, −0.287341, and 2.10798 au, respectively. We note that the location of a secular resonance depends also on eccentricity. However, for the case analysed in this work, all asteroids have $\sin i \lesssim 0.3$ (i.e. $i \lesssim 17°$). The ν_6 secular resonance at these inclinations or smaller is essentially independent of eccentricity (it is almost a straight line as shown by Fig. 6 of Morbidelli & Henrard 1991). On the other hand, for other applications at much higher eccentricities, different approximations of the path of the ν_6 could be needed as function of the eccentricity.

For the lower ($\sin i_{l,j}$) and upper limit ($\sin i_{h,j}$) of each jth-bin of $\sin i$, we compute their corresponding a-values ($a_{l,j}$ and $a_{h,j}$)
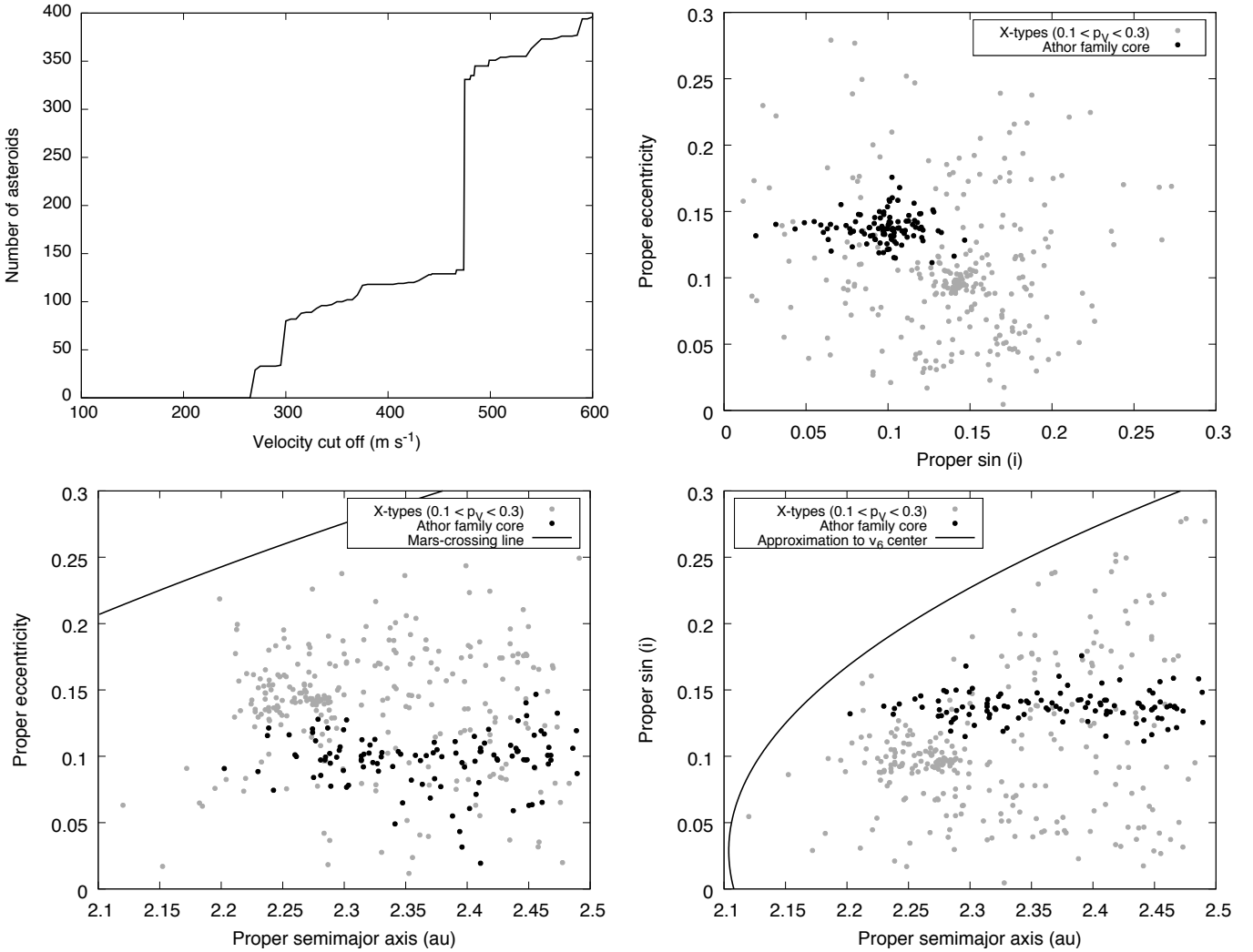
Fig. 4. *Top-left panel*: number of family core members found as a function of velocity cutoff, using the HCM. The second jump in the number of linked asteroids, at 460 m s^{-1}, is our adopted value of velocity cutoff. *Other panels*: distribution of the X-complex asteroid with $0.1 < p_V < 0.3$ of the inner main belt in the three proper elements a, e, $\sin i$. The cluster (of grey points) centred at $(a, e, \sin i) \sim (2.28, 0.144, 0.095\ \mathrm{au})$ is the core of the Baptistina asteroid family.

using Eq. (3); we then compute the area of the trapezium-shaped a space between the ν_6 and the J3:1 MMR of the inclination bin:

$$\mathrm{area}_j = (a_{l,j} - 2.5 + a_{h,j} - 2.5) \times (\sin i_{h,j} - \sin i_{l,j})/2. \tag{4}$$

For each bin in e (and $\sin i$), we count all bodies in a narrow sliver inside of the nominal V shape, that is, with $(a, 1/D)$ verifying the condition $K|a - a_c| \le 1/D \le K|a - a_c| + W$ (where W is small fraction, e.g. 10–20%, of the value of K) and whose values of e (and $\sin i$) are included in each bin. We then multiply the number of asteroids in each bin by the value of e (and $\sin i$) of the centre of the bin and divide by the bin area. The number obtained for each bin is normalised by the total number of asteroids multiplied by the total area. The multiplication by the value of e and $\sin i$ for the eccentricity and the inclination histograms, respectively, is due to the fact that the orbital phase space available to asteroids is proportional to e and $\sin i$.

If the histograms of the normalised e and $\sin i$ distributions have well-defined peaks (see Fig. A.2) – which was not the case for the primordial asteroid family discovered by Delbo et al. (2017) – we denote the coordinates of the peak in eccentricity and inclination as e_c and i_c, respectively.

Subsequently, we use the Hierarchical Clustering Method (HCM; Zappalà et al. 1990) to determine the population that clusters around the family centre. To do so, we create a fictitious asteroid with orbital elements (a_c, e_c, i_c) that we use as central body for the HCM algorithm. We use the HCM version of Nesvorný et al. (2015). We follow this procedure to avoid using real asteroids near the vertex of the family V shape. This is because for old and primordial families, it is possible that the parent asteroid was lost due to the dynamical evolution of the main belt (Delbo et al. 2017; Minton & Malhotra 2010).

The HCM algorithm relies on the "standard metric" of Zappalà et al. (1990, 1995) to calculate a velocity difference between two asteroid orbits. It then connects bodies falling within a cut-off velocity (V_c), creating clusters of asteroids as a function of V_c. The number of asteroids in the cluster N_c is a monotonic growing function of V_c, but as this latter increases the number of family members can grow with steps. For small cut-off velocities no asteroids are linked; when V_c reaches a value appropriate to cluster members of the family, the number of members jumps up, followed by a steady increase of N_c with a further increasing value of V_c, until all family members are linked to each other; if one were to continue increasing V_c,

the value of N_c would jump up again followed by another slow increase. This second jump indicates the limit of the family, because after the jump, the HCM accretes objects outside the family or asteroids belonging to adjacent families. We use the value V_c at the second jump of N_c to define the family. More precisely, we run the HCM for values of V_c between 10 and 600 m s^{-1} with a step of 1 m s^{-1} and we take the minimum value of this parameter to be the nominal V_c of the family, allowing us to link the largest number of asteroids before the second jump in the value of N_c.

4.5. Family age determination

In order to provide an estimate for the age of the family T, and its uncertainty, we use two methods. Firstly, we follow the procedure of Delbo et al. (2017), which is based on the methods of Spoto et al. (2015) that gives an approximate age for the family (as this technique does not take into account the effect of YORP cycles on the Yarkovsky drift of asteroids). The age (T) and its uncertainty are derived from the inverse slope of the V shape given by Eq. (5):

$$1/K = (da/dt)_{1km} \, T, \tag{5}$$

where $(da/dt)_{1km}$ is the rate of change of the orbital proper semi-major axis with time (t) for an asteroid of 1 km in size due to the Yarkovsky effect (Bottke et al. 2006). We perform 10^6 Monte Carlo simulations, where at each iteration, random numbers are obtained from the probability distributions of K and $(da/dt)_{1km}$ in order to be used in Eq. (5). The $(da/dt)_{1km}$ value, obtained by applying the formulas of Bottke et al. (2006), is calculated at each Monte Carlo iteration, and depends on asteroid properties such as the heliocentric distance, infrared emissivity, bolometric Bond albedo (A), thermal inertia, bulk density, rotation period, and obliquity (γ), which is the angle between the spin vector of an asteroid and its orbital plane. The border of the V shape is determined by those asteroids drifting with maximum $|da/dt| \propto \cos\gamma$, meaning that we assume $\gamma = \pm 90°$. For the other parameters, we extract random numbers from their probability distributions. The calculation of the probability distribution for each of the relevant parameters is described in Sect. 5. A change in the luminosity of the Sun as a function of time is taken into account using Eq. (4) of Carruba et al. (2015).

5. Results

We use the V-shape-searching technique on all moderate-albedo X-types of the inner main belt selected as detailed in Sect. 4.1. The result of the V shape search is shown in Fig. 3, where we identify a prominent peak of N_a^2/N_b at $a_c = 2.38$ au and $K = 1.72$ km^{-1} au^{-1}, which we identify with the label "1" in the figure. A further two peaks of N_a^2/N_b at $a_c \sim 2.28$ au and $K \sim 1$ km^{-1} au^{-1} (peak "2" of Fig. 3) and at $a_c = 2.26$ au and $K = 11.9$ km^{-1} au^{-1} are also visible. The latter peak corresponds to the V shape of the Baptistina asteroid family (Nesvorný et al. 2015; Bottke et al. 2007; Masiero et al. 2012b), while the first and second peaks represent previously unknown V shapes (Fig. A.1 gives a graphical representation of the V shapes).

We begin focusing on the V shape centred at $a_c = 2.38$. In order to determine the uncertainties on the values of its a_c and K parameters, we perform a Monte Carlo simulation as described in Sect. 4.2 (the ranges of parameter values explored is $1 \leq K \leq 4$ au^{-1} km^{-1} and $2.34 \leq a_c \leq 2.40$ au). We find that the uncertainties on the determination of a_c and K are 0.006 au and

0.1 au^{-1} km^{-1}, respectively. We note that the average catalogue albedo uncertainty for our pool of asteroids is about 30% relative value, which is similar to the albedo uncertainty estimated by Pravec et al. (2012) for the WISE catalogue.

Subsequently, we study the inclination and eccentricity distributions of those asteroids inside and near the border of the V shape centred at $(a_c, K) = (2.38$ au, 1.72 km^{-1} au$^{-1})$, as detailed in Sect. 4.2. These distributions, presented in Fig. A.2, show maxima at $e_c = 0.12$ and $\sin(i_c) = 0.14$, indicating a potential clustering of objects in (e, i) space. Together with the vertex of the V shape, this information points to a putative centre of the family at $(a_c, e_c, \sin i_c) = (2.38, 0.12, 0.14$ au$)$. We assume a fictitious asteroid with the above-mentioned proper orbital elements for the central body for the HCM algorithm. The latter is used to link asteroids as a function of V_c. Again, we use moderate albedo X-type asteroids of the inner main belt selected as described in Sect. 4.1, as input population for the HCM. The number of asteroids linked by the HCM is displayed in Fig. 4, which shows that $V_c \sim 460$ s^{-1} identifies the second jump in the number of bodies linked to the family as a function of V_c. We thus take this value as the nominal V_c for this cluster. The lowest-numbered and largest asteroid of this cluster is the M-type (161) Athor, which is also the asteroid closest to the vertex of the V shape.

Figure 4 shows that X-type asteroids of the inner main belt have bimodal distributions in e and $\sin i$ with the cluster identified by the HCM and parented by (161) Athor located at high inclination ($\sin i > 0.1$), and low eccentricity ($e \sim 0.1$). Another very diffused group of asteroids appears at low inclination and high eccentricity ($\sin i < 0.1$, $e > 0.12$). Once members of the Baptistina family are removed, most X-type asteroids with $\sin i < 0.1$ and $e > 0.12$ are included inside the V shape defined by $(a_c, K) = (2.38$ au, 1.72 km^{-1} au$^{-1})$, which also borders the HCM cluster of Athor. We make the hypothesis that the group associated to (161) Athor by the HCM is the core of a collisional family and the other asteroids that are within the V shape and have ($\sin i < 0.1$ and $e > 0.12$) form the family "halo" (Parker et al. 2008; Brož & Morbidelli 2013) of the Athor family.

A fundamental test that these two groups of asteroids are members of the same collisional family, dispersed by the Yarkovsky effect, comes from rejecting the null hypothesis that the asteroids semimajor axis could be derived from size-independent distributions. We therefore performed the statistical test described in Sect. 4.3 and find no cases in 10^6 trials where we can generate a V shape like that observed by drawing randomly from the semimajor distribution of all X-type asteroids of the IMB. This demonstrates that the V shape is not just a consequence of the statistical sampling of an underlying size-independent distribution, but is a dispersion of asteroids from a common origin due to the Yarkovsky effect, which is a strong indication that they belong to a collisional family. We use 146 observed bodies, 5 of which are outside the borders of the V shape. The average number of simulated bodies that fall outside the V shape is 23 with a standard deviation of 3.5.

In order to determine the age of the Athor family, as described in Sect. 4.5, we need to estimate the drift rate due to the Yarkovsky effect, which depends on a number of parameters such as heliocentric distance, bulk density, rotation period, and thermal inertia. We fix the semimajor axis at the centre of the family ($a_c = 2.38$ au), and we determine the probability distribution for the albedo, rotational period, density, and thermal inertia, which are all the parameters relevant to estimate the value of da/dt in Eq. (5). Values of the bolometric Bond's albedo (A) are obtained from those of the geometric visible albedo p_V via the equation $A = p_V(0.29 + 0.684G)$, where p_V and G are given

in Table B.1. It is possible to demonstrate that the distribution of A is well approximated by a Gaussian function centred at $A = 0.073$ and with $\sigma = 0.02$. Density has not been calculated for any of the family members. We therefore estimate this parameter by taking a weighted mean density of asteroids belonging to the X complex and with $0.1 \leq p_V \leq 0.3$ (see Table B.4). The weights are given by the inverse square of density uncertainties. We find an average value of 3500 kg m^{-3} and an uncertainty of the mean of 150 kg m^{-3}. We estimate that a value three times larger, that is, 450 kg m^{-3}, is more appropriate for the density uncertainty. For the age determination, we therefore assume that the probability function of the density of family members is a Gaussian function centred at 3500 kg m^{-3} and with $\sigma = 450$ kg m^{-3}. The asteroid (757) Portlandia, with a spherical equivalent diameter of about 33 km, is at the moment of writing the only family member with known thermal inertia value (Γ) around 60 J m^{-2} s$^{-0.5}$ K^{-1} (Hanuš et al. 2018). The other non-family X-complex asteroids with $0.1 < p_V < 0.3$ with measured thermal inertia values are (272) Antonia, (413) Edburga, (731) Sorga, (789) Lena, (857) Glasenappia, and (1013) Tombecka with values of 75, 110, 62, 47, 47, and 55 J m^{-2} s$^{-0.5}$ K^{-1}, respectively, which were measured at heliocentric distances (r_h) of 2.9, 2.9, 3.3, 2.7, 2.3, and 3.1 au, respectively (Hanuš et al. 2018). Since thermal inertia is temperature dependent (Rozitis et al. 2018) and the surface temperature of an asteroid is a function of its heliocentric distance, we correct these thermal inertia values to 2.38 au assuming that $\Gamma \propto r_h^{-3/4}$ (Delbo et al. 2015). We find a mean value of 80 J m^{-2} s$^{-0.5}$ K^{-1} and a standard deviation of 25 J m^{-2} s$^{-0.5}$ K^{-1}. We therefore assume a Gaussian with these parameters for the thermal inertia probability distribution of the family members. We assume the rotation period of family members to be represented by a uniform distribution with values between 2.41 and 6.58 h. This is because the twelve family members with known rotational periods, (757) Portlandia, (2419) Moldavia, (4353) Onizaki, (5236) Yoko, and (7116) Mentall, are very close to the inward border of the family V shape, and are therefore the best candidates to use for the calculation of da/dt due to the Yarkovsky effect. As in the case of the primordial family of Delbo et al. (2017) we find here that the Monte Carlo simulations produce an almost lognormal probability distribution of the ages of the family. The best Gaussian fit to this distribution in log T-space allows us to estimate the most likely age of the family, and its formal standard deviations, to be $3.0^{+0.5}_{-0.4}$ Gyr.

Now, we turn our attention to the "background", that is, those asteroids of the X-type population of the inner main belt with $0.1 < p_V < 0.3$ which remain after we remove the members of the core and halo of the Athor family and the members of the Baptistina family: Fig. 5 shows that their ($a, 1/D$) distribution appears to have a border that follows the outward slope of the V shape with parameters $a_c \sim 2.28$ au and $K \sim 1$ km^{-1} au^{-1}, which corresponds to the peak labelled "2" in Fig. 3.

In order to determine the uncertainties on the values of its a_c and K parameters, we perform a Monte Carlo simulation as described in Sect. 4.2, where the ranges of parameter values explored are $0.0 \leq K \leq 2$ au^{-1} km^{-1} and $2.22 \leq a_c \leq 2.32$ au. We find that the uncertainties on the determination of a_c and K are 0.02 au and 0.2 au^{-1} km^{-1}, respectively.

We perform the statistical test described in Sect. 4.3 and find about 2870 cases in 10^6 trials where we can generate a V shape such as the one observed from a size-independent semimajor axis distribution of asteroids. This demonstrates that this V shape is also probably not just a consequence of the statistical sampling of an underlying size-independent semimajor axis distribution, however with smaller statistical significance than

the V shape of Athor and the V shape of the primordial family of Delbo et al. (2017). We use 183 observed bodies, none of which are outside the borders of the V shape (all the grey points of Fig. 5). The average number of simulated bodies that fall outside the V shape is 4.8 with a standard deviation of 1.8. This means that it is possible that this second V shape is simply due to statistical sampling, despite this probability being very low (~0.29%, which means that this family is robust at 2.98σ). Assuming similar physical properties to those described above, the age ratio between this second V shape and the one centred on (161) Athor is given, to first order, by the ratio of the V-shape slopes, that is, approximately 5.16 Gyr. We refine the age using the same aforementioned Monte Carlo method (taking into account the change of the solar constant with time), and find that the distribution of the family age (t_0) values is well represented by a Gaussian function in $\log_{10}(t_0)$ centred at 0.7 and with a standard deviation of 0.1. This corresponds to a family age of $5.0^{+1.6}_{-1.3}$ Gyr. Given the errors involved in the age estimation process, we conclude that this V shape could be as old as our solar system.

The lowest-numbered asteroid of this V shape is the asteroid (689) Zita with a diameter of 15.6 km, while the largest-numbered member of this family is the asteroid (1063) Aquilegia, which has a diameter of 19 km. We highlight that the CX classification of Zita comes from multi-filter photometry of Tholen & Barucci (1989), and its $p_V = 0.10 \pm 0.02$ is also compatible with an object of the C complex.

6. Discussion

First of all, we advocate caution when dealing with the parenthood of the families, because it is possible that neither (161) Athor nor (689) Zita are the parents of their respective families. This is due to the fact that these families are several gigayears old and have likely lost a significant fraction of their members by collisional and dynamical depletion possibly including their parent bodies or largest remnants (as described by Delbo et al. 2017, and references therein). This is particularly important for the Zita family, which we argue predated the giant planet instability, and to a lesser extent for the Athor family. Some of the Zita family members have sizes of a few kilometres. The lifetime of these bodies in the main belt, before they breakup by collisions, is smaller than the age of the family (Bottke et al. 2005). It is therefore likely that they were created by the fragmentation of a larger Zita family member due to a collision that was more recent than the family-forming one. Fragmentation of bodies inside a family produces new asteroids whose coordinates in the ($a, 1/D$) space still lie inside the family V shape.

Thirteen members of the Athor family have visible spectra from the literature, which we plot in Fig. A.3. Of these, the asteroid (4353) Onizaki has dubious classification and could be a low-albedo S-type (Bus & Binzel 2002), and thus an interloper to this family. The remaining objects have spectra similar to the Xc or the Xk average spectra (Fig. A.3). No family member has near-infrared spectroscopy. Further spectroscopic surveys of members of the Athor family will better constrain the composition of this family (Avdellidou et al., in prep.). In addition, the currently ongoing space mission *Gaia* is collecting low-resolution spectra of asteroids in the visible (Delbo et al. 2012); the *Gaia* Data Release 3 in 2021, will contain asteroid spectra and should help to further constrain family membership.

Fourteen core members of the Athor family – asteroids numbered 2419, 11977, 12425, 17710, 21612, 30141, 30814, 33514, 34545, 42432, 43739, 54169, 68996, and 80599 – and seven
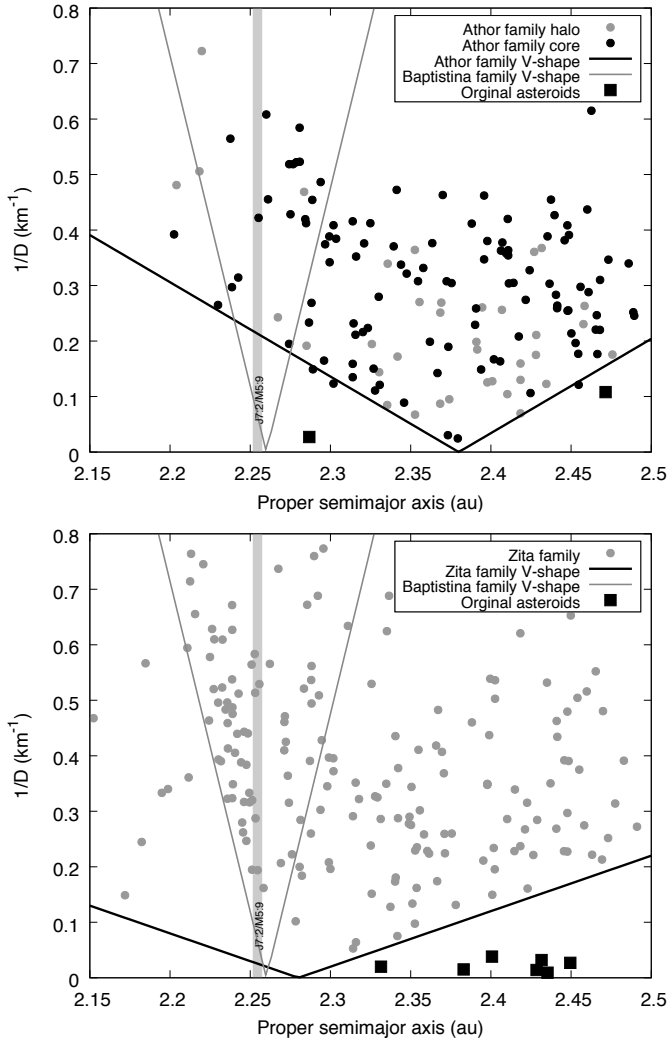
Fig. 5. Distribution of X-complex asteroids with $0.1 < p_V < 0.3$ of the inner main belt in the $(a, 1/D)$ space and that do not belong to the Baptistina asteroid family according to Nesvorný et al. (2015). *Top panel*: asteroids with $\sin i > 0.1$ and $e < 0.12$. Objects represented by circles are Athor family members; the squares are planetesimals. *Bottom panel*: all the other asteroids that belong neither to Baptistina nor the core or halo of Athor. Those represented with circles are Zita family members. Squares are the planetesimals. The position of the overlapping J7:2 MMR and the M5:9 MMR is drawn with a vertical bar. The V shapes of the Hathor, Zita, and Baptistina families are plotted (but not the members of the Baptistina family). As discussed in Sect. 6, we define planetesimals as those asteroids that cannot be included into V shapes.

members of the halo of Athor family – 1697, 2346, 3865, 8069, 29750, 42016, and 79780 – were also linked by Nesvorný et al. (2015) to the family of the asteroid (4) Vesta. None of these asteroids are classified as V-type, which is expected given the composition of (4) Vesta and its family. The geometric visible albedo distribution of these asteroids has a mean value of 0.18 and standard deviation of 0.04, while that of the Vesta family has a mean value of 0.35 and standard deviation of 0.11. The albedo values and spectra or spectrophotometric data of these asteroids are therefore incompatible with those of the Vesta family, making them very likely interlopers that are linked to (4) Vesta by the HCM because of their orbital element proximity. While the V-shape family identification is quite robust against interlopers, in particular because we apply it on compositionally similar

asteroids, the presence of interlopers is still possible. In our case, interlopers are mostly the result of uncertainties in the albedo and spectral identification. We estimated the effect of albedo uncertainty on the selection of asteroids following the Monte Carlo method described in Sect. 4.2. We find that the number of asteroids selected by the criterion $0.1 \leq p_V \leq 0.3$ varies within 6%. Uncertainty in spectral class assignation probably adds another 5–10% to the number of interlopers.

In Fig. 4 one can locate the core of the ν_6 secular resonance at ~2.15 au for $\sin i \sim 0.1$ and Fig. 5 shows that the inward border of the V shape of the Athor family crosses $a = 2.15$ au for $1/D \sim 0.4$ km^{-1}. This implies that the Athor family could feed the ν_6 with asteroids with $D = 2.5$ km or smaller. However, members of the Athor family already start to be removed from the main belt at $a \sim 2.2$ au due to the width of the dynamically unstable region around the ν_6. This indicates that Athor family members with sizes $D \lesssim 2.5$–3 km can leave the main belt and become NEAs. Another possible escape route from the main belt to near-Earth space is the zone of overlapping J7:2 and M5:9 MMR with Jupiter and Mars, respectively (which is also an important escape route for the Baptistina family members; Bottke et al. 2007). Asteroids drifting with $da/dt < 0$ from the centre of the Athor family at $a = 2.38$ au would encounter the overlapping J7:2 and M5:9 MMR before the ν_6. Indeed, the number density of Athor family members visually appears to decrease inward (to the left) of the overlapping J7:2 and M5:9 (Fig. 5). Twelve of the fifteen X-complex NEAs with moderate geometric visible albedo ($0.1 < p_V < 0.3$) have osculating $\sin i > 0.1$, indicating their likely origin from the moderate inclination part of the inner main belt, which is also the location of the Athor family.

Using the aforementioned argument, one can see that the Zita family can deliver asteroids with $1/D \gtrsim 0.12$ km^{-1}, that is, $D \lesssim 8.3$ km, to the ν_6 resonance. Visual inspection of Fig. 5 suggests that the number density of Zita family members firstly increases and then rapidly decreases for $a < 2.2545$ au, where the J7:2 and M5:9 resonances are overlapping. The number density increase is confined within the inward section (i.e. to the left side) of the V shape of the Baptistina family (Fig. 5) despite these asteroids not being linked by Nesvorný et al. (2015) to this family. Out of the 47 asteroids that in Fig. 5 reside between the inward border of the Baptistina family and the J7:2|M5:9 resonances (i.e. those that have $1/D \leq 11.9 \times (a - 2.26)$ km^{-1} and $a < 2.2545$ au), 27 are linked to the Flora asteroid family by Nesvorný et al. (2015). We suspect that these asteroids could in reality be Babptistina family members, although they are currently linked to the Flora family by the HCM of Nesvorný et al. (2015). As in the case of the Athor family, members of the Zita family drifting with $da/dt < 0$ from the centre of the Athor family at $a = 2.28$ au would encounter the overlapping J7:2 and M5:9 MMRs before the ν_6. Both Athor and Zita families can also deliver asteroids of $D \lesssim 5$ km to the near-Earth space via the 3:1 MMR with Jupiter.

While the e and i distributions of the ~3 Gyr-old Athor family are still relatively compact, this is not the case for the Zita family. The e and i distributions of the latter family resemble those calculated by Brasil et al. (2016) during the dynamical dispersal of asteroids – without scattering caused by close encounters with a fifth giant planet – due to the giant planet instability (Tsiganis et al. 2005; Morbidelli et al. 2015). Together with its old age (> 4 Gyr) we interpret the large dispersion in e and i, covering the whole phase space of the inner main belt, as a sign that the Zita family is primordial, that is, it formed
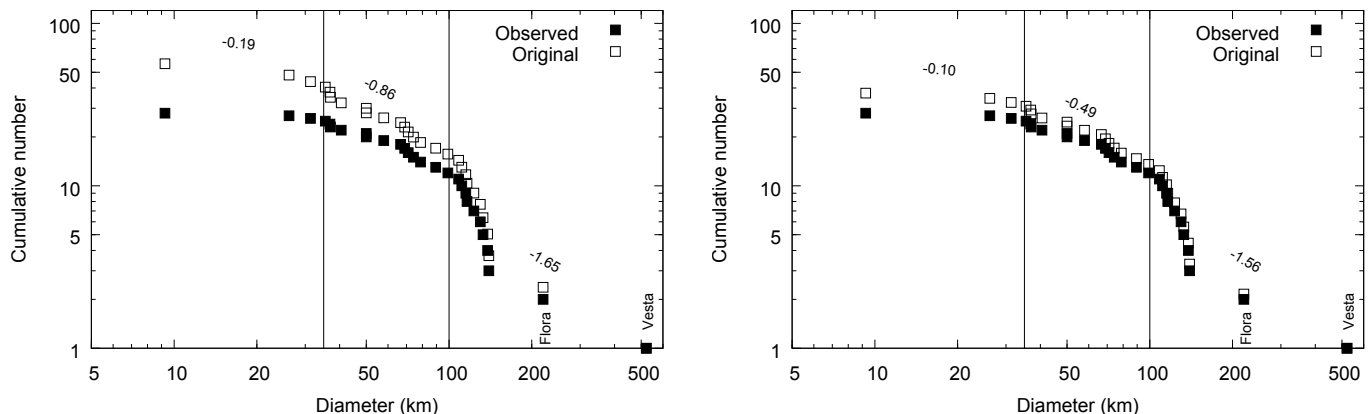
Fig. 6. Cumulative size distribution of planetesimals. This is the cumulative size distribution of those asteroids that are outside V shapes and thus probably do not belong to a family. Additionally, in this dataset, are included the parent bodies of families, as originally they belonged to the planetesimal population. The distribution is then corrected for the maximum number of objects that were lost due the collisional and dynamical evolution; this gives an upper limit for the distribution of the planetesimals (open squares). Functions of the form $N(>D) = N_0 D^\beta$, where N is the cumulative number of asteroids, are fitted piecewise in the size ranges $D > 100$, $35 < D < 100$, and $D < 35$ km. For the original planetesimals size distribution, we obtain the values of β reported by the labels in the plot. *Left panel*: correction to the number of asteroids is calculated taking into account 10 Gyr of collisional evolution in the present main-belt environment, following the prescription of Bottke et al. (2005). *Right panel*: correction to the number of asteroids taking into account 4.5 Gyr of collisional evolution in the present main-belt environment.

before the giant planet instability. This instability is needed to explain the orbital structure of the transneptunian objects (Levison et al. 2008; Nesvorný 2018), the capture of the Jupiter trojans from objects scattered inward from the primordial transneptunian disc (Morbidelli et al. 2005; Nesvorný et al. 2013), the orbital architecture of the asteroid belt (Roig & Nesvorný 2015), and that of the irregular satellites of the giant planets (Nesvorný et al. 2007); see Nesvorný (2018) for a review. The exact timing of this event is still debatable and is a matter of current research: it was initially tied to the Late Heavy bombardment and the formation of the youngest lunar basins, i.e. several hundreds (~700) million years after the formation of the calcium- and aluminium-rich inclusions (Bouvier & Wadhwa 2010; Amelin et al. 2002), which is taken as the reference epoch for the beginning of our solar system. However, recent works tend to invoke an earlier instability (Morbidelli et al. 2018). In addition, simulations by Nesvorný et al. (2018) of the survival of the binary Jupiter Trojan Patroclus–Menoetius, which was originally embedded in a massive transneptunian disc, but dislodged from this and captured as trojan by Jupiter during the instability, indicate that this disc had to be dispersed within less than 100 Myr after the beginning of the solar system. Since the dispersion of the transneptunian disc is a consequence of the giant planet instability (Levison et al. 2008), one can derive the upper limit of 100 Myr for the time for this event (Nesvorný et al. 2018). Moreover, Clement et al. (2018) propose that the instability occurred only a few (1–10) million years after the dispersal of the gas of the protoplantery disc. The age estimate of the Zita family, given its uncertainty, can only constrain the epoch of the giant instability to be ≲600 Myr after the beginning of the solar system. The major source of uncertainty is the determination of the value of da/dt due to the Yarkovsky effect for family members. It is expected that end-of-mission *Gaia* data will allow the Yarkovsky da/dt to be constrained for main-belt asteroids (Gaia Collaboration 2018).

Following the logic of Delbo et al. (2017), we propose that X-complex asteroids with geometric visible albedo between 0.1 and 0.3 of the inner part of the main belt have two populations of bodies: one that comprises the bodies inside V shapes (Athor, Baptistina, and Zita), but not the parent bodies of the families,

and another that includes only those nine bodies that are outside V shapes and the parent bodies of the families: (161) Athor, (298) Baptistina, and (689) Zita. Objects of the former population are family members and were therefore created as fragments of parent asteroids that broke up during catastrophic collisions. On the other hand, asteroids from the latter population cannot be created from the fragmentation of the parent body of a family and as such we consider that they formed as planetsimals by dust accretion in the protoplanetary disc. The implication is that the vast majority of the X-types with moderate albedo of the inner main belt are genetically related to a few parent bodies – Zita, Athor, Hertha (Dykhuis & Greenberg 2015), and possibly Baptistina (Bottke et al. 2007), even though the latter family could be composed by objects whose composition is similar to that of impact-blackened ordinary chondrite meteorites (Reddy et al. 2014) and is therefore more similar to S-type asteroids.

We plot the size distribution of the population of bodies that are not included in V shapes together with those already identified by Delbo et al. (2017) in Fig. 6. As progenitors of the Athor and Zita families, we also add two asteroids whose effective diameters are 133 and 130 km as deduced by the cubic root of the sum of the cube of the diameters of the members of the Athor (core and halo) and Zita families, respectively. These sizes represent a lower limit to the real sizes of the parents that broke up to form the families. Following the same procedure as Delbo et al. (2017) we compute an upper limit for the original size distribution of the planetesimals taking into account asteroid dynamical and collisional loss as a stochastic process. The resulting original size distribution (Fig. 6) is still shallower than predicted by some current accretion models Johansen et al. (2015); Simon et al. (2016), confirming the hypothesis that planetesimals were formed big Morbidelli et al. (2009); Bottke et al. (2005). Compared to previous results (Delbo et al. 2017), which could not find planetesimals smaller than 35 km in diameter, here we identify planetesimals with $D < 35$ km, but the slope of the size distribution of the planetesimals below this latter diameter is very similar to, and even shallower than, the previously computed upper bound (compare Fig. 6 with Figs. 4 and S7 of Delbo et al. 2017).

7. Conclusions

Using our V shape search method (Bolin et al. 2017), we have identified two previously unknown asteroid families in the inner portion of the main belt. These families are found amongst the X-type asteroids with moderate geometric visible albedo ($0.1 < p_V < 0.3$). One of them, the Athor family is found to be ~3 Gyr-old, whereas the second one could be as old as the solar system. The core of the Athor family can be found using the HCM and the distributions of the inclinations, and the eccentricity of the proper orbital elements of its members is relatively compact. On the other hand, in the case of the older family, the eccentricities and inclinations of its member are spread over the entire inner main belt. This is an indication that this family could be primordial, which means that it formed before the giant planet instability.

We show that the vast majority of X-type asteroids of the inner main belt can be included into asteroid families. These asteroids are therefore genetically related and were generated at different epochs from the catastrophic disruption of very few parent bodies. The X-type asteroids with moderate albedo that are not family members in the inner main belt are only nine in number (ten if we include 298 Baptistina). Following the logic of our previous work (Delbo et al. 2017), we conclude that these bodies were formed by direct accretion of the solids in the protoplanetary disc and are thus surviving planetesimals. We combine the planetesimals found in this work with those from our previous study (Delbo et al. 2017) to create a planetesimal size distribution for the inner main belt. After correcting the number of objects due to the size-dependent collisional and dynamical evolution of the main belt, we find that the distribution is steep for $D > 100$ km but it becomes shallower for $D < 100$ km indicating that $D \sim 100$ km was a preferential size for planetesimal formation.

References

Alí-Lagoa, V., & Delbo, M. 2017, A&A, 603, A55
Amelin, Y., Krot, A. N., Hutcheon, I. D., & Ulyanov, A. A. 2002, Science, 297, 1678
Avdellidou, C., Price, M. C., Delbo, M., Ioannidis, P., & Cole, M. J. 2016, MNRAS, 456, 2957
Avdellidou, C., Price, M. C., Delbo, M., & Cole, M. J. 2017, MNRAS, 464, 734
Avdellidou, C., Delbo, M., & Fienga, A. 2018, MNRAS, 475, 3419
Basilevsky, A. T., Head, J. W., Horz, F., & Ramsley, K. 2015, Planet. Space Sci., 117, 312
Binzel, R. P., Reddy, V., & Dunn, T. L. 2015, in Asteroids IV, eds. P. Michel (Tucson: University of Arizona Press), 243
Bolin, B. T., Delbo, M., Morbidelli, A., & Walsh, K. J. 2017, Icarus, 282, 290
Bottke, W. F., Morbidelli, A., Jedicke, R., et al. 2002, Icarus, 156, 399
Bottke, W. F., Durda, D. D., Nesvorný, D., et al. 2005, Icarus, 175, 111
Bottke, W. F. J., Vokrouhlický, D., Rubincam, D. P., & Nesvorný, D. 2006, Ann. Rev. Earth Planet. Sci., 34, 157
Bottke, W. F., Vokrouhlický, D., & Nesvorný, D. 2007, Nature, 449, 48
Bottke, W. F., Brož, M., O'Brien, D. P., et al. 2015a, in Asteroids IV, eds. P. Michel (Tucson: University of Arizona Press), 701
Bottke, W. F., Vokrouhlický, D., Walsh, K. J., et al. 2015b, Icarus, 247, 191
Bouvier, A., & Wadhwa, M. 2010, Nat. Geosci., 3, 637
Brasil, P. I. O., Roig, F., Nesvorný, D., et al. 2016, Icarus, 266, 142
Brož, M., & Morbidelli, A. 2013, Icarus, 223, 844
Brož, M., Morbidelli, A., Bottke, W. F., et al. 2013, A&A, 551, A117
Bus, S. J., & Binzel, R. P. 2002, Icarus, 158, 106
Campins, H., Morbidelli, A., Tsiganis, K., et al. 2010, ApJ, 721, L53
Campins, H., de León, J., Morbidelli, A., et al. 2013, AJ, 146, 26
Carruba, V., Domingos, R. C., Nesvorný, D., et al. 2013, MNRAS, 433, 2075
Carruba, V., Nesvorný, D., Aljbaae, S., & Huaman, M. E. 2015, MNRAS, 451, 244
Carruba, V., Nesvorný, D., Aljbaae, S., Domingos, R. C., & Huaman, M. 2016, MNRAS, 458, 3731
Carry, B. 2012, Planet. Space Sci., 73, 98
Carvano, J. M., Hasselmann, P. H., Lazzaro, D., & Mothé-Diniz, T. 2010, A&A, 510, A43
Clement, M. S., Kaib, N. A., Raymond, S. N., & Walsh, K. J. 2018, Icarus, 311, 340
Ćuk, M., Gladman, B. J., & Nesvorný, D. 2014, Icarus, 239, 154
Delbo, M., Gayon-Markt, J., Busso, G., et al. 2012, Planet. Space Sci., 73, 86
Delbo, M., Mueller, M., Emery, J. P., Rozitis, B., & Capria, M. T. 2015, in Asteroids IV, eds. P. Michel (Tucson: University of Arizona Press), 107
Delbo, M., Walsh, K., Bolin, B., Avdellidou, C., & Morbidelli, A. 2017, Science, 357, 1026
de León, J., Campins, H., Tsiganis, K., Morbidelli, A., & Licandro, J. 2010, A&A, 513, A26
de León, J., Pinilla-Alonso, N., Delbo, M., et al. 2016, Icarus, 266, 57
Delisle, J. B., & Laskar, J. 2012, A&A, 540, A118
DeMeo, F. E., & Carry, B. 2013, Icarus, 226, 723
DeMeo, F. E., Binzel, R. P., Slivan, S. M., & Bus, S. J. 2009, Icarus, 202, 160
DeMeo, F. E., Alexander, C. M. O., Walsh, K. J., Chapman, C. R., & Binzel, R. P. 2015, in Asteroids IV, eds. P. Michel, (Tucson: University of Arizona Press), 13
Dermott, S. F., Christou, A. A., Li, D., Kehoe, T. J. J., & Robinson, J. M. 2018, Nat. Astron., 2, 549
Dykhuis, M. J., & Greenberg, R. 2015, Icarus, 252, 199
Fornasier, S., Migliorini, A., Dotto, E., & Barucci, M. A. 2008, Icarus, 196, 119
Fornasier, S., Clark, B. E., & Dotto, E. 2011, Icarus, 214, 131
Fornasier, S., Lantz, C., Perna, D., et al. 2016, Icarus, 269, 1
Fox, K., Williams, I. P., & Hughes, D. W. 1984, MNRAS, 208, 11P
Gaffey, M. J., Reed, K. L., & Kelley, M. S. 1992, Icarus, 100, 95
Gaia Collaboration (Spoto, F., et al.) 2018, A&A, 616, A13
Granvik, M., Morbidelli, A., Jedicke, R., et al. 2016, Nature, 530, 303
Granvik, M., Morbidelli, A., Vokrouhlický, D., et al. 2017, A&A, 598, A52
Greenstreet, S., Ngo, H., & Gladman, B. 2012, Icarus, 217, 355
Gustafson, B. A. S. 1989, A&A, 225, 533
Hanuš, J., Viikinkoski, M., Marchis, F., et al. 2017, A&A, 601, A114
Hanuš, J., Delbo, M., Durech, J., & Alí-Lagoa, V. 2018, Icarus, 309, 297
Hardersen, P. S., Gaffey, M. J., & Abell, P. A. 2005, Icarus, 175, 141
Hörz, F., & Cintala, M. 1997, Meteor. Planet. Sci., 32, 179
Jewitt, D., Weaver, H., Mutchler, M., Larson, S., & Agarwal, J. 2011, ApJ, 733, L4
Johansen, A., Mac Low, M.-M., Lacerda, P., & Bizzarro, M. 2015, Sci. Adv., 1, 1500109
Lauretta, D. S., Barucci, M. A., Bierhaus, E. B., et al. 2012, Asteroids, Comets, Meteors, No. 229, 2005, eds. D. Lazzaro, S. Ferraz-Mello, & J.A. Fernandez, Proc. IAU Symp., 1667, 6291
Lazzaro, D., Angeli, C. A., Carvano, J. M., et al. 2004, Icarus, 172, 179
Levison, H. F., Morbidelli, A., Van Laerhoven, C., Gomes, R., & Tsiganis, K. 2008, Icarus, 196, 258
Lucas, M. P., Emery, J. P., Pinilla-Alonso, N., Lindsay, S. S., & Lorenzi, V. 2017, Icarus, 291, 268
Mainzer, A., Bauer, J., Grav, T., et al. 2014, ApJ, 784, 110
Masiero, J. R., Mainzer, A. K., Grav, T., et al. 2011, ApJ, 741, 68
Masiero, J. R., Mainzer, A. K., Grav, T., et al. 2012a, ApJ, 759, L8
Masiero, J. R., Mainzer, A. K., Grav, T., Bauer, J. M., & Jedicke, R. 2012b, ApJ, 759, 14
Masiero, J. R., Grav, T., Mainzer, A. K., et al. 2014, ApJ, 791, 121
McCord, T. B., Li, J. Y., Combe, J. P., et al. 2012, Nature, 491, 83
Milani, A., Cellino, A., Knežević, Z., et al. 2014, Icarus, 239, 46
Milani, A., Knežević, Z., Spoto, F., et al. 2017, Icarus, 288, 240
Milić Žitnik, I., & Novaković, B. 2016, ApJ, 816, L31
Minton, D. A., & Malhotra, R. 2010, Icarus, 207, 744
Morate, D., de León, J., De Prá, M., et al. 2016, A&A, 586, A129
Morbidelli, A., & Henrard, J. 1991, Celest. Mech. Dyn. Astron., 51, 131
Morbidelli, A., & Vokrouhlický, D. 2003, Icarus, 163, 120
Morbidelli, A., Levison, H. F., Tsiganis, K., & Gomes, R. 2005, Nature, 435, 462
Morbidelli, A., Bottke, W. F., Nesvorný, D., & Levison, H. F. 2009, Icarus, 204, 558
Morbidelli, A., Walsh, K. J., O'Brien, D. P., Minton, D. A., & Bottke, W. F. 2015, in Asteroids IV eds. P. Michel (Tucson: University of Arizona Press), 493
Morbidelli, A., Nesvorný, D., Laurenz, V., et al. 2018, Icarus, 305, 262

Neese, C. 2010, Asteroid Taxonomy V6.0. EAR-A-5-DDR-TAXONOMY-V6.0. NASA Planetary Data System

Nesvorný, D. 2018, ARA&A, 56, 137

Nesvorný, D., Vokrouhlický, D., & Morbidelli, A. 2007, AJ, 133, 1962

Nesvorný, D., Vokrouhlický, D., & Morbidelli, A. 2013, ApJ, 768, 45

Nesvorný, D., Brož, M., & Carruba, V. 2015, in Asteroids IV, eds. P. Michel, (Tucson: University of Arizona Press), 297

Nesvorný, D., Vokrouhlický, D., Bottke, W. F., & Levison, H. F. 2018, Nat. Astron., 130, 2392

Nugent, C. R., Mainzer, A., Masiero, J., et al. 2015, ApJ, 814, 117

Nugent, C. R., Mainzer, A., Bauer, J., et al. 2016, AJ, 152, 63

Parker, A., Ivezić, Ž., Jurić, M., et al. 2008, Icarus, 198, 138

Popescu, M., Licandro, J., Carvano, J. M., et al. 2018, A&A, 617, A12

Pravec, P., Harris, A. W., Kusnirak, P., Galád, A., & Hornoch, K. 2012, Icarus, 221, 365

Reddy, V., Sanchez, J. A., Bottke, W. F., et al. 2014, Icarus, 237, 116

Roig, F., & Nesvorný, D. 2015, AJ, 150, 186

Rozitis, B., Green, S. F., MacLennan, E., & Emery, J. P. 2018, MNRAS, 477, 1782

Ryan, E. L., & Woodward, C. E. 2010, AJ, 140, 933

Sierks, H., Lamy, P., Barbieri, C., et al. 2011, Science, 334, 487

Simon, J. B., Armitage, P. J., Li, R., & Youdin, A. N. 2016, ApJ, 822, 55

Spoto, F., Milani, A., & Knežević Z. 2015, Icarus, 257, 275

Tedesco, E. F., Noah, P. V., Noah, M., & Price, S. D. 2002, AJ, 123, 1056

Tholen, D. J., & Barucci, M. A. 1989, in Asteroids II, eds. R.P. Binzel, T. Gehrels, & M.S. Matthews (Tucson: The University of Arizona Press), 298

Todorović, N. 2018, MNRAS, 475, 601

Tsiganis, K., Gomes, R., Morbidelli, A., & Levison, H. F. 2005, Nature, 435, 459

Tsirvoulis, G., Morbidelli, A., Delbo, M., & Tsiganis, K. 2018, Icarus, 304, 14

Turrini, D., Svetsov, V., Consolmagno, G., Sirono, S., & Pirani, S. 2016, Icarus, 280, 328

Usui, F., Kuroda, D., Müller, T. G., et al. 2011, PASJ, 63, 1117

Vernazza, P., Binzel, R. P., Thomas, C. A., et al. 2008, Nature, 454, 858

Vernazza, P., Binzel, R. P., Rossi, A., Fulchignoni, M., & Birlan, M. 2009, Nature, 458, 993

Vernazza, P., Castillo-Rogez, J., Beck, P., et al. 2017, AJ, 153, 72

Vokrouhlický, D., Brož, M., Bottke, W. F., Nesvorný, D., & Morbidelli, A. 2006, Icarus, 182, 118

Vokrouhlický, D., Bottke, W. F., & Nesvorný, D. 2017, AJ, 153, 172

Walsh, K. J., Delbo, M., Bottke, W. F., Vokrouhlický, D., & Lauretta, D. S. 2013, Icarus, 225, 283

Warner, B., Harris, Alan, W., & Pravec, P. 2009, Icarus, 202, 134

Williams, I. P., & Wu, Z. 1993, MNRAS, 262, 231

Xu, S., Binzel, R. P., Burbine, T. H., & Bus, S. J. 1995, Icarus, 115, 1

Zappala, V., Farinella, P., Knezevic, Z., & Paolicchi, P. 1984, Icarus, 59, 261

Zappalà, V., Cellino, A., Farinella, P., & Knežević, Z. 1990, AJ, 100, 2030

Zappalà, V., Bendjoya, P., Cellino, A., Farinella, P., & Froeschlé, C. 1995, Icarus, 116, 291

Appendix A: Supplementary figures
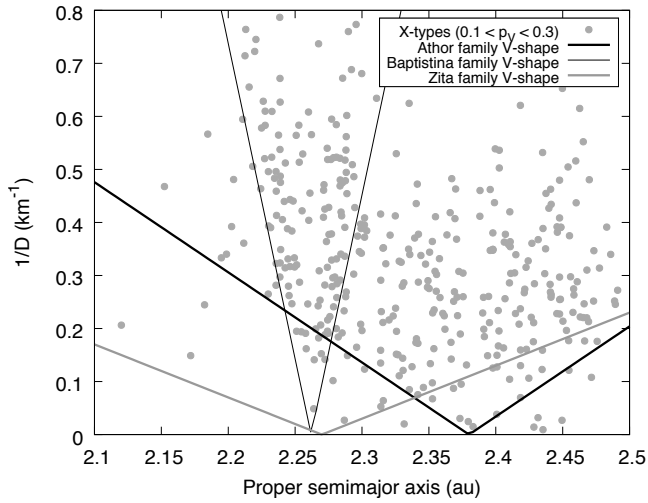
Fig. A.1. V shapes formed by the X-complex asteroids with geometric visible albedos in the range 0.1–0.3 of the inner main belt $(2.1 < a < 2.5 \text{ au})$.
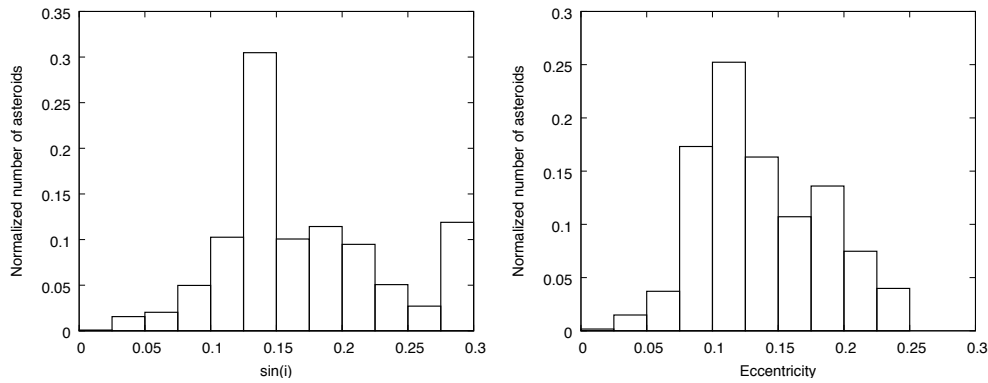
Fig. A.2. Distribution of the proper eccentricity and sinus of the proper inclination for X-type asteroids inside and near the border of the V shape with equation $1/D = 1.72\,|a - 2.38|\ \text{km}^{-1}$ (see text). The peaks show clustering of these asteroids, indicating the centre of the family.
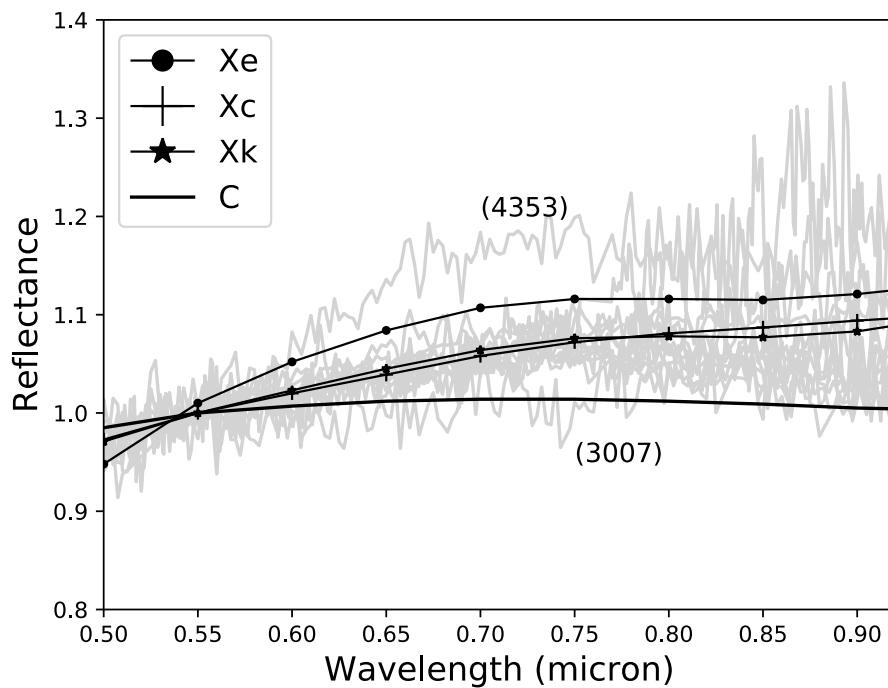
Fig. A.3. Reflectance spectra from the literature of Athor family members numbered 161, 757, 1697, 1998, 2194 3007, 3665, 3704 3865, 4353, 4548, 4839, and 4845. The average reflectance spectra of the Xe, Xc, Xk, and C of the DeMeo et al. (2009) taxonomy (from http://smass.mit.edu/_documents/busdemeo-meanspectra.xlsx) are also plotted. References are: (161) from Bus & Binzel (2002), (757) from Bus & Binzel (2002), 1697 from Xu et al. (1995), (1998) from Bus & Binzel (2002), (2194) from Bus & Binzel (2002), (3007) from Bus & Binzel (2002), 3665 from Xu et al. (1995), (3704) from Bus & Binzel (2002), (3865) from Bus & Binzel (2002), (4353) from Bus & Binzel (2002), (4548) from Bus & Binzel (2002), (4839) from Bus & Binzel (2002), (4845) from Bus & Binzel (2002).

Appendix B: Supplementary tables

Table B.1. Athor family core members.

Number	Designation	a (au)	e	$\sin(i)$	D (km)	σ_D (km)	p_v	σ_{p_V}	P (h)	Taxonomic class	Classi references	D, p_V reference
161	Athor	2.3794	0.0997	0.1535	40.840	0.520	0.233	0.007	7.28	Xc,M	2,4	37
757	Portlandia	2.3732	0.1105	0.1357	32.890	0.240	0.220	0.020	6.58	Xk,XF,X	2,4,6	39
2194	Arpola	2.3278	0.0888	0.1379	9.020	0.040	0.210	0.040	–	Xc,K,X	2,6,7	39
2419	Moldavia	2.2960	0.1045	0.1149	6.070	0.150	0.240	0.030	2.41	C,X	6,7	39
4353	Onizaki	2.3459	0.1016	0.1416	11.240	0.150	0.150	0.030	4.43	Xe,X,X,X	2,3,6,7	39
5160	Camoes	2.4019	0.0606	0.1342	5.984	0.137	0.259	0.075	–	X,X,Cgx	6,7,8	38
5171	Augustesen	2.4247	0.0971	0.1328	9.410	0.330	0.108	0.008	480.00	K,X	6,7	37
5236	Yoko	2.3307	0.1028	0.1372	8.263	0.129	0.151	0.010	2.77	X,S	7,8	38
5343	Ryzhov	2.2742	0.1206	0.1303	5.131	0.076	0.293	0.057	–	X,C	5,6	38
6245	Ikufumi	2.3019	0.1274	0.1512	8.105	0.148	0.129	0.025	–	X	7	38
6247	Amanogawa	2.3939	0.0433	0.1368	6.722	0.098	0.165	0.018	12.38	X,X	6,7	38
6855	Armellini	2.2891	0.0775	0.1345	6.712	0.057	0.125	0.020	–	K,X	6,7	38
7111	1985QA1	2.4058	0.1150	0.1401	6.121	0.056	0.222	0.034	11.21	X,X	6,7	38
7116	Mentall	2.3139	0.1002	0.1397	7.412	0.048	0.152	0.028	6.49	X,X	6,7	38
8381	Hauptmann	2.4664	0.1067	0.1376	5.664	0.032	0.172	0.028	–	C,X,Kl	6,7,8	38
10073	1989GJ2	2.3620	0.0968	0.1364	5.031	0.163	0.233	0.049	–	K,X	6,7	38
11977	Leonrisoldi	2.3269	0.0945	0.1188	6.650	0.190	0.145	0.022	–	X,C	6,7	34
12425	1995VG2	2.3156	0.0920	0.1291	4.730	0.224	0.198	0.019	–	X,C	6,7	38
13101	Fransson	2.4609	0.0653	0.1201	3.470	0.520	0.279	0.072	–	C,CX	6,7	34
14317	Antonov	2.4478	0.1403	0.1163	3.928	0.323	0.262	0.115	–	X,C	6,7	38
15705	Hautot	2.4174	0.1203	0.1381	4.803	0.102	0.160	0.026	–	C,CX	6,7	38
15909	1997TM17	2.2866	0.1213	0.1279	4.286	0.109	0.208	0.011	–	X,X	6,7	38
16007	Kaasalainen	2.3139	0.0968	0.1375	6.291	0.048	0.108	0.020	–	X,C	7,8	38
16258	Willhayes	2.4660	0.0942	0.1371	4.056	0.127	0.129	0.021	–	C,X	6,7	38
17710	1997WT2	2.2843	0.0972	0.1190	2.383	0.345	0.163	0.048	–	S,X	6,7	38
18578	1997XP	2.2386	0.1213	0.1360	3.366	0.059	0.179	0.027	–	X,X	6,7	38
19207	1992QS1	2.3667	0.1005	0.1402	7.022	0.032	0.159	0.020	–	K,X	6,7	38
19473	Marygardner	2.4112	0.1037	0.1340	3.290	0.441	0.236	0.032	–	S,X	6,7	38
19564	Ajburnetti	2.3160	0.1016	0.1316	2.838	0.204	0.166	0.034	–	S,CX	6,7	38
20544	Kimhansell	2.3249	0.1127	0.1470	2.425	0.540	0.228	0.119	–	X	6	38
20566	Laurielee	2.3902	0.1111	0.1427	4.363	0.050	0.185	0.012	–	X,X	6,7	38
20652	1999TY229	2.4545	0.1159	0.1562	5.648	0.144	0.116	0.022	–	K,CX	6,7	38
22761	1998YH4	2.2299	0.0885	0.1378	3.773	0.082	0.197	0.029	–	CX,Xt	7,8	38
24397	Parkerowan	2.4141	0.1099	0.1334	3.280	0.114	0.197	0.039	–	X,X,Kl	6,7,8	38
26660	Samahalpern	2.3233	0.0953	0.1451	4.473	0.166	0.184	0.017	–	X,C	6,7	38
30141	Nelvenzon	2.3958	0.0952	0.1262	2.880	0.614	0.162	0.069	20.74	X,C	6,7	38
30814	1990QW	2.2882	0.1021	0.1290	3.720	0.068	0.243	0.031	–	C,X	6,7	38
33110	1998AM10	2.4528	0.0635	0.1288	5.092	0.163	0.247	0.050	–	C,X	6,7	38
33486	1999GN8	2.4406	0.1036	0.1366	3.530	0.142	0.296	0.040	–	K,X	6,7	38
33514	1999GF34	2.3301	0.0996	0.1213	3.574	0.336	0.166	0.053	–	X,CX,Kl	6,7,8	38
33602	1999JW53	2.4894	0.0870	0.1255	4.072	0.105	0.140	0.041	–	C,X	6,7	38
34061	2000OC48	2.3735	0.0831	0.1475	5.274	0.205	0.160	0.036	–	X,X	6,7	38
34297	2000QH156	2.3724	0.1026	0.1603	3.250	0.547	0.153	0.072	–	X	7	38
34545	2000SB234	2.4414	0.1268	0.1114	3.789	0.140	0.148	0.021	–	X	7	38
34863	2001TP107	2.3202	0.1024	0.1363	4.627	0.150	0.207	0.020	–	C,X,Ad	6,7,8	38
35092	1990WK6	2.3440	0.1036	0.1315	2.961	0.622	0.221	0.129	–	X,X	6,7	38
35739	1999GR21	2.2425	0.0744	0.1394	3.180	0.157	0.132	0.029	–	X,C,Cgx	6,7,8	38
35753	1999GE45	2.4413	0.1039	0.1274	3.859	0.105	0.108	0.021	–	C,X	6,7	38
37983	1998HB136	2.4888	0.1193	0.1482	3.970	0.113	0.135	0.022	–	X,X	6,7	38
38233	1999NS57	2.3144	0.1125	0.1428	4.313	0.024	0.115	0.013	–	K,X	6,7	38
40694	1999RY230	2.4680	0.1007	0.1216	4.543	0.127	0.179	0.041	–	C,X	6,7	38
42432	1134T-3	2.4105	0.1036	0.1152	2.381	0.612	0.113	0.074	–	X	7	38
42633	1998FW58	2.3546	0.0820	0.1478	3.248	1.118	0.265	0.115	–	X,X	6,7	38

References. (1) DeMeo et al. (2009); (2) Bus & Binzel (2002), (3) Xu et al. (1995), (4) Tholen & Barucci (1989), (5) Lazzaro et al. (2004), (6) DeMeo & Carry (2013), (7) Carvano et al. (2010), (8) Popescu et al. (2018), (32) Nugent et al. (2016), (33) Nugent et al. (2015), (34) Masiero et al. (2012a), (35) Tedesco et al. (2002), (36) Ryan & Woodward (2010), (37) Usui et al. (2011), (38) Masiero et al. (2011), (39) Masiero et al. (2014), (70) Mainzer et al. (2014), (71) Alí-Lagoa & Delbo (2017).

Table B.1. continued.

Number	Designation	a (au)	e	$\sin(i)$	D (km)	σ_D (km)	p_v	σ_{p_V}	P (h)	Taxonomic class	Classi reference	D, p_V reference
43120	1999XB49	2.4366	0.1002	0.1401	3.296	0.078	0.148	0.028	–	X	7	38
43656	2002ER104	2.4217	0.1010	0.1576	3.646	0.223	0.160	0.017	3.22	X,C	6,7	38
43739	1981EP7	2.3755	0.1050	0.1259	3.285	0.687	0.149	0.072	–	X,X	6,7	38
43845	1993OS9	2.4242	0.0980	0.1327	3.053	0.743	0.250	0.135	–	C,CX	6,7	38
44983	1999VU163	2.4063	0.0963	0.1388	2.755	0.601	0.233	0.075	–	CX	7	38
54169	2000HF57	2.3394	0.0923	0.1288	2.698	0.301	0.243	0.063	–	C,CX	6,7	38
54196	2000HH78	2.4483	0.1306	0.1354	3.919	0.169	0.138	0.028	–	X	7	38
56627	2000JF84	2.3475	0.0649	0.1403	3.111	0.137	0.152	0.008	–	X,C	6,7	38
56674	2000KS77	2.4095	0.0802	0.1423	2.791	0.943	0.189	0.079	–	C,CX	6,7	38
58177	1990TB6	2.3035	0.0782	0.1233	2.602	0.459	0.238	0.078	–	X	7	38
63081	2000WP133	2.4502	0.0630	0.1369	4.678	0.183	0.169	0.025	–	CX	7	38
65642	1981ES2	2.2939	0.0993	0.1372	2.056	0.553	0.264	0.101	–	S,X	6,7	38
67449	2000QQ166	2.4072	0.0713	0.1552	2.648	0.553	0.230	0.175	–	X	6	38
67583	2000SZ120	2.4559	0.1467	0.1284	3.360	0.191	0.188	0.047	–	C,X	6,7	38
68425	2001QS329	2.3019	0.0767	0.1370	2.447	0.884	0.141	0.062	–	X,C	6,7	38
68750	2002EM68	2.2887	0.0948	0.1499	2.201	0.078	0.100	0.004	–	CX	7	38
68996	2002TN135	2.2993	0.0893	0.1315	2.574	0.561	0.184	0.149	–	X	7	38
70332	1999RF166	2.3978	0.0919	0.1454	2.630	0.437	0.147	0.079	–	K,CX	6,7	38
70363	1999RJ193	2.4108	0.0194	0.1317	2.822	0.884	0.128	0.073	–	K,X	6,7	38
70899	1999VS176	2.4681	0.0971	0.1359	3.224	0.517	0.246	0.042	–	CX	7	38
74119	1998QH52	2.4547	0.0916	0.1410	8.250	1.850	0.266	0.267	–	X,X	6,7	34
80418	1999XA206	2.2025	0.0908	0.1320	2.550	0.665	0.156	0.095	–	C,X	6,7	38
80599	2000AB148	2.2848	0.0994	0.1256	2.425	0.767	0.208	0.164	–	C,X,Kl	6,7,8	38
80835	2000DK7	2.3908	0.1024	0.1758	3.865	0.242	0.171	0.043	–	L,X	6,7	38
82121	2001FQ77	2.3139	0.0975	0.1341	2.405	0.564	0.211	0.109	–	C,X	6,7	38
82690	2001PB34	2.3579	0.1007	0.1422	3.015	0.814	0.194	0.056	–	C,C,Xt	6,7,8	38
85175	1990RS	2.2995	0.1200	0.1484	2.924	0.760	0.227	0.093	–	C,X	6,7	38
85611	1998HW16	2.4375	0.0590	0.1398	2.199	0.579	0.175	0.093	–	X,CX	6,7	38
88506	2001QW140	2.3210	0.1085	0.1353	2.659	0.671	0.228	0.144	–	C,CX	6,7	38
92599	2000PR19	2.3635	0.0789	0.1351	2.656	0.266	0.158	0.023	–	X,Kl	7,8	38
92949	2000RS41	2.4654	0.1007	0.1588	4.533	0.185	0.180	0.024	–	X	6	38
94674	2001XK21	2.4487	0.0974	0.1477	2.557	0.794	0.246	0.181	–	X,X	6,7	38
95733	2003DG22	2.2808	0.0972	0.1486	1.711	0.294	0.240	0.090	–	X,C	6,7	38
95873	2003GH37	2.3958	0.0316	0.1403	2.164	0.177	0.137	0.044	–	C,CX	6,7	38
98028	2000RJ5	2.2809	0.0856	0.1331	1.912	0.360	0.253	0.123	–	X,C	6,7	38
98239	2000SH156	2.2552	0.1162	0.1432	2.370	0.695	0.125	0.030	–	X,X,Kl	6,7,8	38
99490	2002CD220	2.2743	0.1179	0.1417	1.928	0.389	0.207	0.090	–	K,X	6,7	38
101262	1998SU104	2.3413	0.0490	0.1415	2.117	0.224	0.273	0.085	–	K,X	6,7	38
105551	2000RW46	2.3881	0.0550	0.1424	2.429	0.643	0.131	0.044	–	X	7	38
105909	2000SZ201	2.4108	0.1061	0.1423	2.750	0.150	0.102	0.008	–	C,X	6,7	38
108866	2001OO99	2.4460	0.0974	0.1496	2.621	0.495	0.135	0.066	–	X,X	6,7	38
110342	2001SN292	2.4397	0.1060	0.1374	2.343	0.548	0.154	0.067	–	X,X	6,7	38
119194	2001QH109	2.2611	0.0998	0.1370	2.196	0.254	0.175	0.045	–	X,C	6,7	38
119357	2001SM238	2.4859	0.1060	0.1584	2.943	0.792	0.141	0.059	–	C,X	6,7	38
124848	2001TZ15	2.2787	0.1279	0.1496	1.915	0.160	0.192	0.065	–	L,X	6,7	38
125003	2001TV154	2.4353	0.1083	0.1246	2.573	0.445	0.184	0.050	–	X	7	38
125100	2001UA34	2.2751	0.0840	0.1351	2.334	0.351	0.155	0.053	–	X,X	6,7	38
125337	2001VE51	2.3700	0.0685	0.1377	2.159	0.365	0.165	0.157	–	X	7	38
125764	2001XG136	2.2967	0.1071	0.1680	2.672	0.478	0.130	0.037	–	C,X	6,7	38
125895	2001XX212	2.4477	0.0972	0.1350	2.448	0.437	0.186	0.108	–	X	7	38
126771	2002DU15	2.4733	0.1325	0.1341	2.885	0.378	0.193	0.080	–	CX	7	38
132277	2002EV150	2.4601	0.1192	0.1372	2.288	0.586	0.194	0.087	–	X	7	38
145964	1999YY7	2.2376	0.1156	0.1317	1.771	0.163	0.246	0.021	–	X,C	6,7	38
208206	2000ST24	2.2600	0.1011	0.1455	1.644	0.296	0.216	0.044	–	K,X	6,7	38
232377	2003BN13	2.2767	0.1117	0.1306	1.928	0.319	0.109	0.049	–	X,CX	6,7	38
243637	Frosinone	2.3785	0.0771	0.1339	1.508	0.313	0.195	0.079	–	CX	7	38
264495	2001QB10	2.4627	0.1168	0.1381	1.626	0.378	0.202	0.102	–	CX	7	38

Table B.2. Athor family halo members.

Number	Designation	a (au)	e	$\sin(i)$	D (km)	σ_D (km)	p_v	σ_{p_V}	P (h)	Taxonomic class	Class references	D, p_V reference
1490	Limpopo	2.3527	0.0951	0.1911	14.840	0.110	0.170	0.030	6.65	Xc	2	39
1697	Koskenniemi	2.3741	0.1145	0.1057	10.520	0.660	0.150	0.021	–	TX	3	37
1998	Titius	2.4185	0.0848	0.1355	14.340	0.220	0.100	0.040	6.13	Xc,C,C	2,6,7	39
2015	Kachuevskaya	2.3354	0.1023	0.2098	11.810	0.150	0.140	0.020	42.53	X,C	6,7	39
3007	Reaves	2.3684	0.0921	0.1321	11.468	0.052	0.147	0.022	4.16	X	2	38
3665	Fitzgerald	2.4185	0.1112	0.2520	7.690	1.770	0.200	0.120	2.41	X,C,X	3,6,7	33
3704	Gaoshiqi	2.4103	0.0552	0.1149	9.580	0.070	0.210	0.040	9.77	Xk	2	39
3865	Lindbloom	2.3978	0.0938	0.1230	7.972	0.068	0.181	0.019	–	Xc	2	38
4548	Wielen	2.2851	0.0965	0.1354	5.220	0.090	0.179	0.030	–	Xc,S	2,6	38
4760	Jia-xiang	2.3258	0.0785	0.1754	5.137	0.036	0.228	0.042	–	X,X	6,7	38
4839	Daisetsuzan	2.4346	0.0369	0.1328	8.141	0.099	0.202	0.032	–	Xc	2	38
4845	Tsubetsu	2.4009	0.0825	0.1248	7.838	0.052	0.182	0.027	–	X	2	38
6123	Aristoteles	2.3304	0.0276	0.1678	6.946	0.066	0.164	0.020	–	X,X	6,7	38
7447	Marcusaurelius	2.3910	0.0751	0.1270	5.034	0.122	0.220	0.010	–	Xt	8	38
8069	Benweiss	2.3418	0.1060	0.1057	5.812	0.037	0.185	0.047	–	L,DL,Xt	6,7,8	38
10368	Kozuki	2.3915	0.0814	0.1727	5.412	0.063	0.200	0.055	–	X,X	6,7	38
13274	Roygross	2.4584	0.0354	0.1393	3.798	0.171	0.134	0.017	–	CX	7	38
20508	1999RL25	2.4758	0.0652	0.2791	5.689	0.113	0.198	0.022	–	X,X	6,7	38
24053	Shinichiro	2.2183	0.0737	0.1154	1.977	0.343	0.216	0.065	6.21	X	7	38
29750	Chleborad	2.4281	0.0836	0.1103	5.714	0.062	0.155	0.010	–	Xt	8	38
33616	1999JR64	2.4185	0.1163	0.2469	6.269	0.125	0.149	0.021	–	X	7	38
36398	2000OQ45	2.4283	0.0908	0.2002	4.740	0.120	0.198	0.019	–	X,C	6,7	38
42016	2000YZ68	2.3946	0.1178	0.1071	3.838	0.143	0.120	0.012	–	X,X	6,7	38
42920	1999SA8	2.2672	0.1191	0.1027	4.120	0.950	0.130	0.070	4.90	CX	7	32
49869	1999XG115	2.2040	0.0825	0.1100	2.079	0.385	0.178	0.106	–	CX	7	38
61224	2000OO13	2.3685	0.0396	0.1125	3.980	0.129	0.161	0.034	–	Xt	8	38
67993	2000XD24	2.3526	0.0117	0.1577	2.746	0.778	0.195	0.149	–	X	7	38
71788	2000ST180	2.2836	0.0420	0.1423	2.133	0.615	0.245	0.197	–	C,X	6,7	38
72799	2001FC188	2.4577	0.0317	0.2220	4.339	0.218	0.113	0.016	–	S,X,S	6,7,8	38
79780	1998US37	2.3357	0.1181	0.1114	2.946	0.642	0.154	0.052	–	X,Ad	7,8	38
102416	1999TL184	2.3555	0.0237	0.2298	3.700	0.110	0.107	0.023	–	L,Xt	7,8	34
102808	1999VG172	2.4317	0.0825	0.1764	2.720	0.629	0.137	0.093	–	C,X	6,7	38
116046	2003WZ102	2.4270	0.0841	0.2495	2.773	0.122	0.252	0.054	–	Xt	8	38
122409	2000QE89	2.4069	0.0631	0.1829	3.903	0.155	0.168	0.022	–	X,X	6,7	38
184012	2004FT12	2.3691	0.0783	0.2386	3.714	0.176	0.106	0.016	–	CX	7	38
243735	2000OT1	2.2198	0.0833	0.1605	1.384	0.237	0.211	0.091	–	X	7	38

Notes. For references see Table B.1.

Table B.3. Zita family members.

Number	Designation	a (au)	e	$\sin(i)$	D (km)	σ_D (km)	p_v	σ_{p_V}	P (h)	Taxonomic class	Class references	D, p_V reference
689	Zita	2.3159	0.1878	0.0956	15.620	0.230	0.100	0.020	6.43	CX	4	39
1063	Aquilegia	2.3141	0.0795	0.0937	18.930	0.370	0.139	0.006	5.79	X,K,X	3,6,7	37
2233	Kuznetsov	2.2783	0.0775	0.0719	9.830	0.660	0.153	0.021	5.03	K,X	6,7	37
2328	Robeson	2.3417	0.2007	0.1749	13.300	0.460	0.105	0.008	18.63	C,C,X	2,6,7	37
2968	Iliya	2.3714	0.2729	0.1689	4.460	0.960	0.130	0.080	–	C,X,Cgx	6,7,8	33
2991	Bilbo	2.3374	0.1968	0.0704	7.818	0.147	0.115	0.013	4.06	Ch,X,C	5,6,7	38
3137	Horky	2.4009	0.1835	0.0589	6.685	0.089	0.207	0.030	–	C,X,CX	2,6,7	38
3375	Amy	2.1719	0.0909	0.0290	6.721	0.118	0.124	0.005	3.26	C,X,C	2,6,7	38
3427	Szentmartoni	2.2808	0.1080	0.0552	5.003	0.070	0.224	0.034	–	Xt	8	38
3461	Mandelshtam	2.3781	0.1170	0.0423	7.615	0.097	0.160	0.017	2.85	X,XL	6,7	38
4095	Ishizuchisan	2.1201	0.0631	0.0546	4.845	0.204	0.189	0.027	–	S,S,Xt	6,7,8	38
4256	Kagamigawa	2.3511	0.0516	0.0393	7.480	0.070	0.230	0.020	–	Xc	2	39
4838	Billmclaughlin	2.3526	0.1461	0.1628	10.250	0.190	0.140	0.010	5.20	Xc	2	39
6182	Katygord	2.2546	0.1822	0.1006	5.158	0.051	0.185	0.024	–	X,X	6,7	38
7739	Cech	2.3251	0.1682	0.0567	4.196	0.091	0.174	0.046	–	X,X	6,7	38
9388	Takeno	2.2476	0.1599	0.0684	4.053	0.345	0.129	0.013	–	C,CX,Xt	6,7,8	38
9602	Oya	2.2822	0.1166	0.0390	5.436	0.076	0.165	0.024	–	X,X	6,7	38
9735	1986JD	2.3537	0.1694	0.1383	6.172	0.085	0.168	0.040	–	S,X	6,7	38
10309	1990QC6	2.3278	0.1702	0.0046	3.058	0.428	0.273	0.077	–	Xt	8	38
10359	1993TU36	2.4229	0.1291	0.1672	6.217	0.165	0.263	0.038	2.41	X	7	38
10991	Dulov	2.3539	0.1917	0.0530	4.252	0.028	0.162	0.022	–	C,X	6,7	38
11286	1990RO8	2.3756	0.1657	0.0540	3.848	0.050	0.191	0.014	14.81	C,X	6,7	38
12177	Raharto	2.3978	0.1194	0.0434	2.864	0.436	0.236	0.043	–	X,XD	6,7	38
12582	1999RY34	2.2511	0.1612	0.0346	5.134	0.147	0.243	0.059	–	Xt	8	38
14026	Esquerdo	2.3604	0.1451	0.0437	4.377	0.194	0.111	0.010	–	X,C	6,7	38
14413	Geiger	2.2878	0.1348	0.0976	3.848	0.274	0.227	0.054	–	C,CX	6,7	38
14505	Barentine	2.3583	0.2040	0.0428	3.870	0.186	0.155	0.021	2.89	X,L	6,7	38
14950	1996BE2	2.2583	0.1504	0.1022	6.180	0.050	0.190	0.030	3.28	C,X	6,7	39
15793	1993TG19	2.4102	0.1862	0.0637	3.497	0.926	0.132	0.092	22.40	CX	7	38
15996	1998YC12	2.3000	0.1772	0.1398	5.099	0.157	0.142	0.025	–	X,X	6,7	38
16177	Pelzer	2.3711	0.1389	0.0422	3.857	0.262	0.157	0.024	–	S,X	6,7	38
16273	Oneill	2.2990	0.0905	0.0765	4.807	0.049	0.133	0.017	–	X,D	6,7	38
16821	1997VZ4	2.2691	0.1483	0.1011	4.838	0.083	0.171	0.016	–	C,X	6,7	38
16967	Marcosbosso	2.2938	0.1211	0.0628	3.304	0.101	0.194	0.031	–	X,C	6,7	38
17635	1996OC1	2.4024	0.1199	0.0997	5.117	0.166	0.107	0.024	–	X	6	38
18866	1999RA208	2.4265	0.1741	0.2095	4.520	0.128	0.286	0.036	–	C,X,Kl	6,7,8	38
19531	Charton	2.2496	0.1421	0.1091	3.164	0.130	0.101	0.013	–	X	7	38
19633	Rusjan	2.4456	0.2105	0.2211	4.385	0.297	0.277	0.096	–	Xt	8	38
20458	1999LZ21	2.3421	0.1780	0.1160	3.478	0.167	0.111	0.017	–	X	7	38
21091	1992DK8	2.2455	0.1381	0.1034	3.816	0.043	0.138	0.014	–	K,CX	6,7	38
21475	Jasonclain	2.1823	0.0648	0.0419	4.086	0.144	0.127	0.027	–	X,D	6,7	38
22459	1997AD2	2.3257	0.0740	0.0808	6.600	1.000	0.100	0.030	–	X,CX	6,7	71
22571	Letianzhang	2.2388	0.1536	0.0955	3.090	0.670	0.120	0.060	–	X,C	6,7	33
23996	1999RT27	2.3707	0.1705	0.0505	2.714	0.398	0.182	0.066	–	Xt	8	38
25037	1998QC37	2.1987	0.2186	0.0884	2.940	0.670	0.210	0.090	–	C,X,Ds	6,7,8	33
26014	2051P-L	2.4485	0.1760	0.0597	2.560	0.340	0.186	0.052	–	X,CX	6,7	34
26082	1981EB11	2.4458	0.1758	0.0623	2.552	0.497	0.226	0.101	–	C,X	6,7	38
26226	1998GJ1	2.3615	0.0407	0.0777	4.466	0.140	0.185	0.047	–	X	7	38
27043	1998RS71	2.1949	0.0758	0.0970	3.000	0.200	0.196	0.021	–	X	7	38
27740	Obatomoyuki	2.3953	0.1742	0.1792	4.736	0.195	0.261	0.055	–	X,C	6,7	38
28046	1998HB14	2.3407	0.1526	0.1922	5.536	0.348	0.174	0.029	–	X,X	6,7	38
28805	2000HY85	2.4289	0.1581	0.0916	3.515	0.130	0.299	0.041	–	C,X	6,7	38
29442	1997NS4	2.3978	0.1357	0.1631	2.877	0.531	0.234	0.084	–	C,CX	6,7	38
29652	1998WD9	2.3313	0.1423	0.1524	3.494	0.244	0.145	0.031	–	CX	7	38
29660	Jessmacalpine	2.2928	0.1680	0.0565	1.965	0.442	0.240	0.091	–	X,C	6,7	38
30244	Linhpham	2.2116	0.1774	0.1144	2.770	0.820	0.130	0.090	–	X,C,S	6,7,8	32

Notes. For references see Table B.1.

Table B.3. continued.

Number	Designation	a (au)	e	$\sin(i)$	D (km)	σ_D (km)	p_v	σ_{p_V}	P (h)	Taxonomic class	Class references	D, p_V reference
30777	1987SB3	2.2450	0.1348	0.0945	3.574	0.290	0.152	0.036	–	X,C	6,7	38
30819	1990RL2	2.3403	0.1873	0.1741	5.763	0.037	0.101	0.023	–	C,X	6,7	38
31110	Clapas	2.2716	0.1772	0.0671	2.122	0.068	0.171	0.031	–	S,X	6,7	38
31682	Kinsey	2.4213	0.0864	0.0917	3.740	0.194	0.200	0.048	–	C,X	6,7	38
31902	Raymondwang	2.2243	0.1394	0.0534	2.157	0.374	0.263	0.088	–	S,S,Xt	6,7,8	38
31937	Kangsunwoo	2.2302	0.1516	0.0894	2.542	0.005	0.191	0.060	–	C,CX	6,7	38
32079	Hughsavoldelli	2.2476	0.1329	0.1233	2.605	0.033	0.223	0.020	–	K,CX	6,7	38
33234	1998GL7	2.3665	0.1877	0.2377	5.748	0.198	0.112	0.034	–	L,X	6,7	38
33454	1999FJ27	2.3157	0.1483	0.0743	2.844	0.652	0.218	0.085	–	C,CX	6,7	38
33528	Jinzeman	2.3348	0.1664	0.0630	2.860	0.159	0.113	0.035	–	X	7	38
33595	1999JC49	2.4731	0.1220	0.0316	3.972	0.106	0.123	0.022	–	X	7	38
33597	1999JQ49	2.3882	0.1621	0.0228	2.173	0.435	0.236	0.103	–	X	7	38
33901	2000KJ56	2.4693	0.1683	0.1756	4.695	0.105	0.184	0.044	–	K,X	6,7	38
34120	2000PL28	2.3659	0.1810	0.1168	2.390	0.577	0.235	0.095	–	C,X	6,7	38
34779	Chungchiyung	2.2813	0.1311	0.1115	3.516	0.079	0.143	0.024	–	X,Ds	7,8	38
35160	1993NY	2.3140	0.1386	0.0370	3.435	0.062	0.111	0.033	–	CX	7	38
36455	2000QZ6	2.4911	0.2493	0.2771	3.673	0.907	0.131	0.049	–	X,C	6,7	38
36881	2000SX154	2.4147	0.1397	0.1793	4.381	0.163	0.278	0.038	–	C,X	6,7	38
37723	1996TX28	2.4829	0.0796	0.0951	2.556	0.613	0.296	0.188	–	Xt	8	38
37738	1996VM14	2.4410	0.1708	0.0174	2.161	0.441	0.287	0.115	–	K,X	6,7	38
37982	1998HB132	2.4775	0.0199	0.0828	3.185	0.709	0.209	0.058	–	C,X	6,7	38
38155	1999JJ69	2.2712	0.1843	0.0915	2.440	0.082	0.297	0.044	–	X	6	38
38810	2000RP70	2.4631	0.1231	0.0373	4.509	0.207	0.115	0.038	–	C,X	6,7	38
39038	2000UE80	2.3528	0.1366	0.0779	4.360	0.052	0.156	0.022	–	C,X	6,7	38
39108	2000WG26	2.3293	0.1695	0.0702	3.077	0.102	0.107	0.027	–	X,X	6,7	38
41817	2000WX40	2.2533	0.1305	0.1163	3.480	0.340	0.231	0.059	–	Xt	8	34
42960	1999TJ139	2.4184	0.1339	0.0334	1.611	0.144	0.205	0.042	–	S,X	6,7	38
43282	2000EB140	2.2392	0.1268	0.1027	2.867	0.067	0.163	0.015	–	CX	7	38
43387	2000WF58	2.2990	0.1870	0.0867	2.520	0.389	0.254	0.099	–	X	7	38
46603	1993FY41	2.4226	0.1257	0.0321	3.170	0.380	0.146	0.039	–	X,CX	6,7	34
49701	1999VZ1	2.2108	0.1295	0.0308	1.682	0.160	0.207	0.043	–	X,CX	6,7	38
49874	1999XW129	2.2405	0.1501	0.1206	2.467	0.301	0.201	0.050	–	C,CX	6,7	38
49911	1999XT169	2.4184	0.2244	0.0788	4.216	0.293	0.208	0.030	–	C,CX	6,7	38
50228	2000AD242	2.4582	0.1655	0.1725	3.640	0.290	0.193	0.037	–	S,X	6,7	34
51440	2001FW24	2.2980	0.2377	0.1250	2.898	0.587	0.175	0.090	–	X	7	38
52328	1992EK11	2.4026	0.1753	0.0878	1.865	0.289	0.292	0.062	–	S,CX	6,7	38
52441	1994RS1	2.3990	0.2436	0.1702	2.287	0.058	0.281	0.045	–	X	7	38
53625	2000CZ96	2.1523	0.0170	0.0862	2.138	0.581	0.293	0.120	–	CX	7	38
53977	2000GM70	2.2461	0.1614	0.1099	3.156	0.076	0.173	0.013	–	X,C,Ad	6,7,8	38
54103	2000HX6	2.4414	0.1772	0.0466	2.303	0.246	0.192	0.039	–	CX	7	38
54355	2000KJ33	2.2760	0.1604	0.1173	4.496	0.054	0.139	0.009	–	X	7	38
54419	2000LA20	2.4018	0.2234	0.2246	4.275	0.017	0.283	0.021	–	X,X	6,7	38
55374	2001SE244	2.4551	0.0908	0.0267	2.667	0.718	0.108	0.077	–	X	7	38
55467	2001TH173	2.2872	0.1905	0.0297	2.559	0.135	0.142	0.011	–	S,X,S	6,7,8	38
55663	6247P-L	2.2880	0.1119	0.0697	1.864	0.284	0.202	0.051	–	X,C	6,7	38
56374	2000EM24	2.2262	0.1615	0.0880	1.591	0.277	0.211	0.056	–	X	7	38
56408	2000FH22	2.1847	0.0624	0.0983	1.765	0.242	0.248	0.042	–	C,X	6,7	38
56651	2000KH46	2.2388	0.1279	0.0940	1.595	0.504	0.159	0.065	–	K,X,V	6,7,8	38
57434	2001SH46	2.3178	0.1978	0.0384	3.105	0.927	0.183	0.149	–	S,X	6,7	38
58336	1994VP	2.2722	0.1820	0.1140	2.352	0.226	0.153	0.089	–	X	7	38
58598	1997TX11	2.2946	0.1499	0.0630	2.336	0.104	0.186	0.036	–	X,CD,Kl	6,7,8	38
59024	1998SB106	2.3109	0.1720	0.0513	1.577	0.485	0.214	0.087	–	C,X	6,7	38
59239	Alhazen	2.2512	0.1888	0.1195	3.125	0.661	0.181	0.145	–	X,C	6,7	38
59397	1999FT26	2.4372	0.1758	0.0460	2.855	0.192	0.198	0.021	–	X,CX	6,7	38
60540	2000EZ61	2.2557	0.1522	0.0931	1.890	0.467	0.136	0.056	–	C,X	6,7	38
60665	2000FL73	2.4540	0.1669	0.0421	1.982	0.356	0.284	0.068	–	S,L,Xt	6,7,8	38
60916	2000JL37	2.2494	0.1309	0.1157	3.001	0.421	0.215	0.071	–	C,X	6,7	38
63380	2001HE51	2.4598	0.0729	0.0919	1.938	0.560	0.225	0.133	–	C,X	6,7	38

Table B.3. continued.

Number	Designation	a (au)	e	$\sin(i)$	D (km)	σ_D (km)	p_v	σ_{p_V}	P (h)	Taxonomic class	Class references	D, p_V reference
65745	1993TT31	2.2675	0.1545	0.0425	1.357	0.321	0.241	0.092	–	Xt	8	38
67411	2000QJ26	2.2855	0.1261	0.1076	1.488	0.225	0.241	0.050	–	CX	7	38
67597	2000SA141	2.2427	0.1365	0.0923	1.953	0.476	0.140	0.094	–	C,X	6,7	38
67639	2000SE216	2.2508	0.1952	0.1092	1.772	0.404	0.170	0.047	–	X	7	38
68550	2001XA54	2.3365	0.1876	0.0396	1.453	0.266	0.277	0.050	–	X,X	6,7	38
68836	2002GU105	2.4477	0.1770	0.2158	4.398	0.145	0.110	0.027	–	X	7	38
70125	1999NZ	2.3502	0.1375	0.1778	3.632	0.084	0.102	0.013	–	X,X	6,7	38
75374	1999XG84	2.4477	0.1434	0.1902	3.368	0.080	0.171	0.026	–	Xt	8	38
75660	2000AG77	2.4408	0.1509	0.0760	3.722	0.207	0.127	0.041	–	C,X	6,7	38
78647	2002TQ48	2.2443	0.1833	0.0929	2.576	0.525	0.184	0.050	–	X	7	38
80650	2000AY246	2.2359	0.1652	0.0883	2.179	0.570	0.162	0.102	–	C,CX	6,7	38
82676	2001PV23	2.3489	0.2670	0.1286	3.600	0.500	0.140	0.040	–	X,CX,Kl	6,7,8	71
86797	2000GM108	2.2317	0.1584	0.0998	2.563	0.061	0.269	0.033	–	X,V	7,8	38
86799	2000GH112	2.2346	0.1529	0.0802	2.069	0.320	0.217	0.043	–	X	7	38
88629	2001RQ34	2.2462	0.1370	0.0672	2.256	0.317	0.166	0.094	–	X,D	6,7	38
90084	2002VC116	2.3493	0.2362	0.1351	3.446	0.061	0.196	0.025	–	C,X	6,7	38
90102	2002XQ21	2.2741	0.2260	0.0672	3.170	0.159	0.133	0.045	–	X	7	38
90115	2002XJ54	2.2327	0.0957	0.0777	1.641	0.215	0.238	0.071	–	C,CX	6,7	38
91242	1999CX32	2.3018	0.1701	0.1472	2.529	0.099	0.230	0.047	–	C,X	6,7	38
91309	1999FB55	2.3557	0.1740	0.1729	3.313	0.605	0.161	0.059	–	C,X	6,7	38
92324	2000GE49	2.2156	0.1344	0.1056	1.526	0.172	0.209	0.034	–	X	7	38
92537	2000OS16	2.2419	0.1539	0.1268	2.275	0.324	0.215	0.035	–	X	7	38
94688	2001XL27	2.3978	0.1563	0.2051	2.864	0.413	0.236	0.080	–	Xt	8	38
96288	1996GD6	2.2389	0.1340	0.0940	2.052	0.438	0.116	0.040	–	C,CX	6,7	38
96349	1997US7	2.2485	0.1238	0.0169	2.271	0.318	0.124	0.032	–	X,CX	6,7	38
96651	1999GT62	2.3549	0.1458	0.1379	2.434	0.143	0.156	0.035	–	X,C,C	6,7,8	38
98089	2000RO72	2.2882	0.1698	0.0753	2.023	0.342	0.188	0.064	–	X	7	38
98123	2000SG15	2.2272	0.1222	0.0820	1.922	0.243	0.158	0.058	–	C,CX	6,7	38
98352	2000SX327	2.3422	0.1509	0.0780	2.647	0.637	0.191	0.076	–	X,C	6,7	38
98383	2000TL39	2.2361	0.1475	0.1178	2.420	0.691	0.190	0.092	–	X,C	6,7	38
99650	2002HF2	2.2882	0.0366	0.0552	1.780	0.298	0.202	0.061	–	X,Ad	7,8	38
103600	2000CM16	2.2358	0.1351	0.1051	3.099	0.691	0.106	0.043	–	S,X	6,7	38
105983	2000SE269	2.2713	0.1634	0.1039	2.170	0.242	0.164	0.049	–	S,X	6,7	38
109038	2001QC13	2.4699	0.1665	0.0502	2.081	0.355	0.195	0.056	–	X,C,Ad	6,7,8	38
111483	2001YZ38	2.2276	0.1354	0.0960	1.640	0.382	0.165	0.089	–	S,X	6,7	38
112019	2002GL168	2.2531	0.0755	0.0908	1.947	0.211	0.107	0.031	–	X	7	38
120005	2002YB31	2.3768	0.1792	0.0440	1.478	0.272	0.203	0.062	–	X,XL	6,7	38
121951	2000ES45	2.3505	0.2060	0.1770	2.907	0.858	0.120	0.064	–	X	7	38
129428	4164T-3	2.2734	0.1144	0.0681	2.747	0.599	0.123	0.092	–	X,CX	6,7	38
130744	2000SH259	2.2835	0.0964	0.0447	1.919	0.456	0.132	0.061	–	CX	7	38
132366	2002GF68	2.4026	0.1823	0.1937	1.989	0.536	0.234	0.191	–	K,X	6,7	38
136797	1997CF1	2.2131	0.1994	0.1346	1.309	0.386	0.179	0.101	–	X	7	38
137818	2000AR3	2.4150	0.1685	0.2391	2.948	0.047	0.117	0.015	–	X,D	6,7	38
145882	1999TU32	2.2207	0.1623	0.0446	1.342	0.100	0.270	0.071	–	X,C	6,7	38
148158	1999XB153	2.2357	0.1478	0.0907	2.016	0.379	0.158	0.045	–	C,CX	6,7	38
149614	2004EP11	2.2300	0.1295	0.0884	2.017	0.256	0.109	0.044	–	CX	7	38
155998	2001RQ21	2.2387	0.1016	0.0211	1.860	0.111	0.128	0.016	–	X	7	38
158611	2003AY35	2.2622	0.1694	0.0720	1.768	0.237	0.118	0.045	–	X,C	6,7	38
161242	2003BK13	2.3695	0.1559	0.1780	2.456	0.088	0.106	0.019	–	X,C	6,7	38
162528	2000QT134	2.2325	0.1317	0.1109	1.912	0.409	0.192	0.126	–	X,C	6,7	38
166079	2002CW102	2.3256	0.2166	0.0512	1.888	0.507	0.180	0.108	–	X,C	6,7	38
167102	2003SB47	2.4350	0.1960	0.1293	1.880	0.616	0.165	0.098	–	S,CX	6,7	38
188198	2002RX59	2.2528	0.1600	0.0872	1.714	0.241	0.218	0.126	–	C,X,S	6,7,8	38
193024	2000ET60	2.2387	0.1800	0.0998	1.489	0.335	0.182	0.104	–	X,C	6,7	38
194798	2001YW97	2.3405	0.1800	0.0580	2.296	0.180	0.160	0.026	–	X	7	38
215473	2002RZ50	2.2390	0.1574	0.1151	2.103	0.472	0.159	0.071	–	K,X	6,7	38
222425	2001OV	2.4498	0.1977	0.1232	1.532	0.426	0.189	0.104	–	X	7	38
227423	2005VC42	2.4477	0.1247	0.1882	2.085	0.270	0.162	0.029	–	CX	7	38

Table B.3. continued.

Number	Designation	a (au)	e	$\sin(i)$	D (km)	σ_D (km)	p_v	σ_{p_V}	P (h)	Taxonomic class	Class references	D, p_V reference
234143	2000EY44	2.2249	0.1424	0.0985	1.730	0.353	0.135	0.040	–	C,X	6,7	38
235005	2003CW17	2.2143	0.1567	0.0951	1.210	0.200	0.121	0.042	–	CX	7	34
235039	2003FN40	2.3352	0.1436	0.0690	1.601	0.309	0.131	0.049	–	X	7	38
240308	2003FP100	2.2898	0.1288	0.0874	1.316	0.296	0.147	0.053	–	K,X	6,7	38
240319	2003HU37	2.3019	0.1711	0.1901	2.687	0.148	0.117	0.011	–	Xt	8	38
241921	2002AG186	2.4654	0.1489	0.1727	1.811	0.422	0.135	0.035	–	C,CX	6,7	38
242248	2003ST233	2.3996	0.2654	0.1682	1.856	0.413	0.117	0.018	–	X,L,S	6,7,8	38
243780	2000SC20	2.3671	0.1808	0.1366	2.072	0.436	0.124	0.055	–	X	7	38
253490	2003SJ91	2.2921	0.1289	0.0969	1.453	0.248	0.121	0.061	–	X,X	6,7	38
276825	2004PM101	2.2125	0.1955	0.1549	1.400	0.200	0.120	0.040	–	C,X	6,7	71
423025	2003TB21	2.2956	0.1517	0.1054	1.293	0.253	0.116	0.029	–	C,CX	6,7	38

Table B.4. Known densities and their uncertainties of asteroids of the X complex and with $0.1 < p_V < 0.3$.

Asteroid	Density kg m^{-3}	1σ kg m^{-3}	Ref.
16 Psyche	3700	600	a
15 Eunomia	3500	400	b
21 Lutetia	3400	300	c
22 Kalliope	3700	400	a
69 Hesperia	4400	1000	d
97 Klotho	4200	600	d
129 Antigone	2500	900	a
135 Hertha	4500	700	a
216 Kleopatra	5000	700	a
516 Amherstia	8000	7600	d
665 Sabine	9100	5200	d
758 Mancunia	2700	300	d

Notes. Those asteroids with unrealistic densities, marked with a cross in the Table 1 of Carry (2012) are not included.
References. (a) Hanuš et al. (2017), (b) Avdellidou et al. (2018), (c) Sierks et al. (2011), (d) Carry (2012).

Table B.5. Original asteroids i.e. the surviving planetesimals.

Number	Designation	a (au)	e	$\sin(i)$	D (km)	σ_D (km)	p_v	σ_{p_V}	P (h)	Taxonomic class	Class references	D, p_V reference
4	Vesta	2.3615	0.0988	0.1113	521.740	7.500	0.342	0.013	5.34	V,V,V	1,2,4	37
8	Flora	2.2014	0.1449	0.0971	147.490	1.030	0.230	0.040	12.86	Sw,S	1,4	39
18	Melpomene	2.2958	0.1802	0.1701	139.590	2.450	0.230	0.030	11.57	S,S,S	1,2,4	39
51	Nemausa	2.3657	0.1140	0.1740	138.160	0.970	0.100	0.030	7.78	Cgh,Ch,CU	1,2,4	39
654	Zelinda	2.2970	0.2130	0.3165	116.300	2.380	0.050	0.010	31.74	Ch,C	2,4	39
12	Victoria	2.3343	0.1751	0.1624	115.090	1.200	0.160	0.030	8.66	L,S,D	2,4,5	39
27	Euterpe	2.3470	0.1865	0.0123	114.100	4.480	0.220	0.030	10.41	S,S,S,L	1,2,4,5	39
40	Harmonia	2.2673	0.0216	0.0654	111.250	0.390	0.220	0.050	8.91	S,S,S	1,2,4	39
345	Tercidina	2.3253	0.0987	0.1799	99.000	11.469	0.059	0.012	12.37	Ch,Ch,C	1,2,4	38
326	Tamara	2.3176	0.2034	0.3943	89.420	1.510	0.040	0.002	14.44	C	4	37
72	Feronia	2.2662	0.0741	0.1037	78.800	2.000	0.080	0.010	8.10	STD,TDG	3,4	39
80	Sappho	2.2960	0.1508	0.1620	74.250	3.000	0.210	0.010	14.03	S,S	2,4	39
336	Lacadiera	2.2518	0.0882	0.1071	69.000	3.364	0.046	0.005	13.70	Xk,D	2,4	38
207	Hedda	2.2840	0.0656	0.0589	57.880	0.150	0.060	0.010	30.10	Ch,C,Ch	2,4,5	39
261	Prymno	2.3315	0.1311	0.0512	50.010	0.520	0.140	0.030	8.00	X,B	2,4	39
136	Austria	2.2868	0.0183	0.1732	36.890	0.520	0.220	0.050	11.50	Xe,M	2,4	39
376	Geometria	2.2886	0.1712	0.1064	35.470	0.050	0.320	0.050	7.74	Sl,S,S,S	2,4,6,7	39
298	Baptistina	2.2639	0.1476	0.1038	20.530	0.270	0.170	0.005	16.23	Xc	5	37
21	Lutetia	2.4353	0.1292	0.0374	108.380	1.280	0.181	0.005	8.17	Xc,Xk,M,X	1,2,4,5	37
131	Vala	2.4316	0.0940	0.0721	31.340	0.300	0.170	0.040	5.18	K,Xc,CX,SU	1,2,3,4	39
135	Hertha	2.4285	0.1741	0.0466	71.040	2.650	0.180	0.030	8.40	Xk,M	2,4	39
261	Prymno	2.3315	0.1311	0.0512	50.010	0.520	0.140	0.030	8.00	X,B	2,4	39
337	Devosa	2.3830	0.1569	0.1391	66.630	0.980	0.127	0.005	4.65	Xk,X,X	1,2,4	37
435	Ella	2.4495	0.1212	0.0287	37.040	0.500	0.106	0.003	4.62	DCX	4	37
572	Rebekka	2.4007	0.1358	0.1854	26.190	0.370	0.111	0.004	5.65	C,XDC,C,C	2,4,6,7	37
13977	Frisch	2.4715	0.0797	0.2768	9.260	0.110	0.160	0.020	5.00	X,X	6,7	39

Notes. The first group in the table is from Delbo et al. (2017). The second from this work. For references see Table B.1.